

# Image Differential Invariants

Hanlin Mo<sup>1,2</sup> · Hua Li<sup>1,2</sup>

Received: date / Accepted: date

**Abstract** Inspired by the methods of systematic derivation of image moment invariants, we design two fundamental differential operators to generate image differential invariants for the action of 2D Euclidean, similarity and affine transformation groups. Each differential invariant obtained by using the new method can be expressed as a homogeneous polynomial of image partial derivatives. When setting the degree of the polynomial and the order of image partial derivatives are less than or equal to 4, we generate all Euclidean differential invariants and discuss the independence of them in detail. In the experimental part, we find the relation between Euclidean differential invariants and Gaussian-Hermite moment invariants when using the derivatives of Gaussian to estimate image partial derivatives. Texture classification and image patch verification are carried out on some synthetic and popular real databases. We mainly evaluate the stability and discriminability of Euclidean differential invariants and analyse the effects of various factors on performance of them. The experimental results validate image Euclidean differential invariants have better performance than some commonly used local image features in most cases.

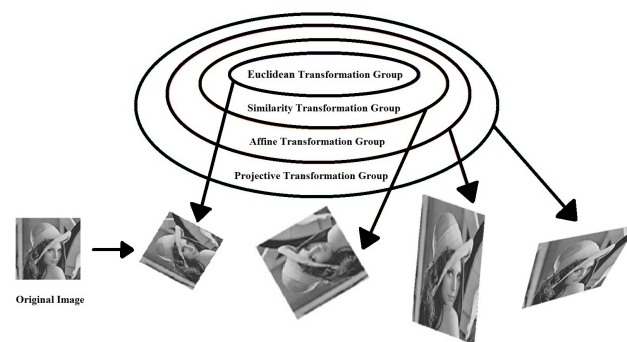


Fig. 1: The relation between commonly used transformation groups

**Keywords** Differential invariants · Moment invariants · Local image structure · Image verification · Texture classification

## 1 Introduction

The geometric deformation of a planar object caused by the change of viewpoints can be modeled with 2D Euclidean, similarity, affine or projective transformation group. The relation between these groups is shown in Fig. 1. In order to correctly recognize planar objects, researchers have designed many methods to extract image invariant features for the action of various 2D transformation groups. Image moment invariants and differential invariants are two of them.

Image moments are integrals of an image with basis functions. Image moment invariants are formed by taking algebraic combinations of image moments. Usually, they are used to describe global image structure. In 1962, Hu employed the theory of algebraic invariants to generate seven image similarity moment invariants (Hu

Hanlin Mo ✉  
E-mail: mohanlin@ict.ac.cn

Hua Li  
E-mail: lihua@ict.ac.cn

<sup>1</sup> Key Laboratory of Intelligent Information Processing, Institute of Computing Technology, Chinese Academy of Sciences, Beijing, China

<sup>2</sup> University of Chinese Academy of Sciences, Beijing, China

1962). Since then, many achievements have been made in the theory of image moment invariants (Flusser and Suk 1993; Li et al. 2017; Xu and Li 2008), and hundreds of papers have been devoted to their application in many fields (Heikkilä 2004; Karakasis et al. 2015). At present, the research on them mainly focuses on three aspects.

The first one is to construct image moment invariants for the action of more complicated transformation groups. In 1993, Reiss (1991) and Flusser and Suk (1993) independently proposed the method to derive image affine moment invariants. Nearly thirty years later, Li and Mo (2018) proved the existence of image projective moment invariants using finite combinations of weighted moments, with relative projective differential invariants as weight functions. The second one is to define image moments using various orthogonal basis functions, such as Zernike moments (Teague et al. 1980), Fourier-Mellin moments (Sheng and Shen 1994), Tchebichef moments (Mukundan et al. 2001) and Gaussian-Hermite moments (Yang and Dai 2011; Yang et al. 2011). Due to the property of orthogonality, they are widely used for image reconstruction. The third aspect is to design the method of systematic derivation of image moment invariants. In 2005, Suk and Flusser (2004) presented a graph method for generating affine moment invariants. Then, Xu and Li (2008) found some geometric primitives, such as distance, area and volume, can be used to construct similarity and affine moment invariants. Recently, Li et al. (2017) proposed these geometric primitives can be replaced with two fundamental generating functions.

Image differential invariants can be expressed as the functions of image partial derivatives. Unlike image moment invariants, they are widely used to describe local image structures. In fact, before being applied in computer vision and pattern recognition, the general theory of differential invariants has been studied by mathematicians for many years (Lie 1884). In the 19th century, Cartan (1935) proposed that the method of moving frames can be employed to generate differential invariants for the action of various transformation groups. Olver et al. developed this method and obtained some differential invariants in explicit forms (Calabi et al. 1998; Olver 1995; Olver et al. 1999; Olver 1999; Olver 2015). Koenderink and Florack et al. discussed image differential invariants in detail and proposed the method to derive the complete and irreducible set of image Euclidean differential invariants (Koenderink and van Doorn 1987; Koenderink and van Doorn 1992; Salden et al. 1992; Florack et al. 1992; Florack et al. 1993; Florack et al. 1994; Ter Haar Romeny et al. 1994; Florack and Balmashnova 2008). However, it is

difficult to systematically generate differential invariants using these methods. Recently, Li et al. (2017) found the isomorphism between differential and moment invariants under affine transform, which means image affine differential invariants can be derived from image affine moment invariants by substituting moments by partial derivatives of the same order.

Inspired by Li's discovery and the methods of systematic derivation of image moment invariants, we first design two fundamental differential operators in this paper and apply them to generate image differential invariants for the action of 2D Euclidean, similarity and affine transformation groups. Each invariant obtained using the new method can be expressed as the homogeneous polynomial of image partial derivatives.

Then, when setting the degree of the homogeneous polynomial and the order of image partial derivatives are less than or equal to 4, we generate all Euclidean differential invariants and obtain the linearly independent set, irreducible set and functional independent set of them. Although we don't find the general method to generate differential invariants for the action of more complicated 2D transformation groups, some image projective and conformal differential invariants can be found from these Euclidean ones.

Finally, we test the performance of image Euclidean differential invariants in the experimental part. When using the derivatives of Gaussian to estimate image partial derivatives, we find the relation between Gaussian-Hermite moment invariants and Euclidean differential invariants. The classification experiments on eight synthetic databases are carried out. Based on the results, we discuss the effects of various factors on the performance of Euclidean differential invariants in detail. Also, we conduct image verification and texture classification experiments on popular real databases. Some famous handcrafted image features are chosen for comparison, such as SIFT, LBP and so on. And the results show that image differential invariants have better performance than others in most cases.

## 2 Basic Concepts and Definitions

In this section, we introduce basic concepts and definitions that we will use in the following sections.

### 2.1 Commonly Used Image Transformation Groups

As shown in Fig. 1, 2D Euclidean, similarity, affine and projective transformations are commonly used image deformation models. Suppose the image function  $f(x, y) : \Omega \subset \mathbb{N}^+ \times \mathbb{N}^+ \rightarrow \mathbb{R}$  is transformed to  $h(u, v) :$

$\Omega' \subset \mathbb{N}^+ \times \mathbb{N}^+ \rightarrow \mathbb{R}$  using a 2D transformation  $g$ .  $(u, v) \in \Omega'$  is the corresponding point of  $(x, y)$  and  $h(u, v) = f(x, y)$ .

If  $g$  belongs to 2D Euclidean transformation group, the relation between  $(u, v)$  and  $(x, y)$  is:

$$\begin{pmatrix} u \\ v \end{pmatrix} = \begin{pmatrix} \cos \theta & -\sin \theta \\ -\sin \theta & \cos \theta \end{pmatrix} \begin{pmatrix} x \\ y \end{pmatrix} + \begin{pmatrix} t_1 \\ t_2 \end{pmatrix} \quad (1)$$

Ignoring the translation  $(t_1, t_2)^T$ ,  $\theta$ , the angle of rotation, can completely determine the 2D Euclidean transformation.

If  $g$  is a 2D similarity transformation, we have:

$$\begin{pmatrix} u \\ v \end{pmatrix} = \begin{pmatrix} s \cdot \cos \theta & -s \cdot \sin \theta \\ -s \cdot \sin \theta & s \cdot \cos \theta \end{pmatrix} \begin{pmatrix} x \\ y \end{pmatrix} + \begin{pmatrix} t_1 \\ t_2 \end{pmatrix} \quad (2)$$

Note that the matrix in Eq.(2) is composed of 2D rotation (Angle  $\theta$ ) and isotropic scaling (Scale factor  $s$ ).

If  $g$  belongs to 2D affine transformation group,  $(u, v)$  can be obtained by using:

$$\begin{pmatrix} u \\ v \end{pmatrix} = \begin{pmatrix} a & b \\ c & d \end{pmatrix} \begin{pmatrix} x \\ y \end{pmatrix} + \begin{pmatrix} t_1 \\ t_2 \end{pmatrix} \quad (3)$$

where  $(ad - bc) \neq 0$ . Actually, the matrix in Eq.(3) can be composed of 2D rotation, anisotropic scaling and shear. Thus,  $g$  contains six independent parameters.

If  $g$  is a 2D projective transformation, we have:

$$u = \frac{ax + by + t_1}{px + qy + r} \quad v = \frac{cx + dy + t_2}{px + qy + r} \quad (4)$$

In this case,  $g$  is a nonlinear transformation and contains eight independent parameters. If both  $p$  and  $q$  are zeros, it becomes a 2D affine transformation. In fact, it has been proven that 2D projective transformation group can simulate all geometric deformations of a planar object caused by the change of viewpoints. When the size of the object is much smaller than the distance between itself and the camera, these deformations can also be modeled by 2D affine transformation group.

## 2.2 Image Partial Derivatives and Local Jet

Suppose the image function  $f(x, y)$  is infinitely differential at the point  $(x_0, y_0)$  in its domain. The Taylor series about  $(x, y) = (x_0 + \Delta x, y_0 + \Delta y)$  is the power series:

$$\begin{aligned} f(x, y) = & f(x_0, y_0) + \frac{\partial f}{\partial x} \Delta x + \frac{\partial f}{\partial y} \Delta y + \frac{1}{2!} \left( \frac{\partial^2 f}{\partial x^2} \Delta x^2 \right. \\ & + 2 \frac{\partial^2 f}{\partial x \partial y} \Delta x \Delta y + \frac{\partial^2 f}{\partial y^2} \Delta y^2 \left. \right) + \frac{1}{3!} \left( \frac{\partial^3 f}{\partial x^3} \Delta x^3 \right. \\ & + 3 \frac{\partial^3 f}{\partial x^2 \partial y} \Delta x^2 \Delta y + 3 \frac{\partial^3 f}{\partial x \partial y^2} \Delta x \Delta y^2 \\ & \left. + \frac{\partial^3 f}{\partial y^3} \Delta y^3 \right) + \dots \end{aligned}$$

$$(5)$$

where  $\frac{\partial^{i+j} f}{\partial x^i \partial y^j}$  denotes the  $(i+j)$ th order partial derivative at  $(x_0, y_0)$ . We can find  $f(x, y)$  in the neighborhood of  $(x_0, y_0)$  can be described by its partial derivatives.

However, we can not calculate the exact value of  $\frac{\partial^{i+j} f}{\partial x^i \partial y^j}$  at  $(x_0, y_0)$  because  $\Omega$ , the domain of the image function  $f(x, y)$ , is a discrete set. But, given a scale factor  $\sigma$ , we can estimate it by convolving  $f(x, y)$  with  $(i+j)$ th order partial derivative of 2D Gaussian function:

$$L_{ij}(x_0, y_0; \sigma) = f \otimes \sigma^{i+j} \cdot \frac{\partial^{i+j} G(x, y; \sigma)}{\partial x^i \partial y^j} \quad (6)$$

where  $\otimes$  denotes convolution and  $G(x, y; \sigma) = \frac{1}{2\pi\sigma^2} \cdot e^{-\frac{(x-x_0)^2 + (y-y_0)^2}{2\sigma^2}}$ . Based on this method, the local jet of order  $N$  at the point  $(x_0, y_0)$  is defined by:

$$J^N(x_0, y_0; \sigma) = \{L_{10}(x_0, y_0; \sigma), L_{01}(x_0, y_0; \sigma), \dots, L_{N0}(x_0, y_0; \sigma), \dots, L_{0N}(x_0, y_0; \sigma)\} \quad (7)$$

When  $N \rightarrow \infty$ ,  $J^N(x_0, y_0; \sigma)$  contains all information of the image  $f(x, y)$  in the neighborhood of the point  $(x_0, y_0)$ .

## 2.3 Image Local Structure and Differential Invariant

Local structure is intrinsic property of an image. It will be unchanged under various 2D transforms defined in Sec.2.1. Suppose the image function  $f(x, y)$  is transformed to  $h(u, v)$  using Eq.(1). We can find that

$$\begin{aligned} \frac{\partial h}{\partial u} &= \cos \theta \cdot \frac{\partial f}{\partial x} + \sin \theta \cdot \frac{\partial f}{\partial y} \\ \frac{\partial h}{\partial v} &= -\sin \theta \cdot \frac{\partial f}{\partial x} + \cos \theta \cdot \frac{\partial f}{\partial y} \end{aligned} \quad (8)$$

Although the local structure in the neighborhood of  $(x, y)$  is invariant under 2D Euclidean transform, partial derivatives have changed. Thus, they can not represent image local structure. In order to solve this problem, image differential invariants are constructed based on the partial derivatives of  $f(x, y)$ .

Let  $DI$  be a function of image partial derivatives and  $G$  be a 2D transformation group. Suppose  $f(x, y)$  is transformed to  $h(u, v)$  using  $g \in G$ .  $DI$  is an image differential invariant for the action of  $G$  iff:

$$\begin{aligned} \forall g \in G : DI(h, \frac{\partial h}{\partial u}, \frac{\partial h}{\partial v}, \frac{\partial^2 h}{\partial u^2}, \frac{\partial^2 h}{\partial u \partial v}, \frac{\partial^2 h}{\partial v^2}, \dots) \\ = w(x, y; g) \cdot DI(f, \frac{\partial f}{\partial x}, \frac{\partial f}{\partial y}, \frac{\partial^2 f}{\partial x^2}, \frac{\partial^2 f}{\partial x \partial y}, \frac{\partial^2 f}{\partial y^2}, \dots) \end{aligned} \quad (9)$$

When  $w(x, y; g) \equiv 1$ ,  $DI$  is an absolute invariant, otherwise it is a relative invariant. In this paper, we suppose

$DI$  is the homogeneous polynomial of image partial derivatives. In fact, Florack et al. (1993) have proved that all non-polynomial differential invariants can be expressed as the functions of homogeneous polynomial ones. The order of  $DI$  is, by definition, the maximum order of partial derivative it depends upon. And its degree is the highest degree of monomials in  $DI$ .

#### 2.4 Image Geometric Moment Invariants

Geometric moment invariants are most well-known image moment invariants. For the continuous function  $f(x, y) : \Omega \subset \mathbb{R} \times \mathbb{R} \rightarrow \mathbb{R}$ , the  $(i+j)$ th order geometric moment is defined by:

$$\mu_{ij}^f = \iint_{\Omega} x^i y^j f(x, y) dx dy \quad (10)$$

where  $i, j \in \{0, 1, 2, \dots\}$ . In order to achieve translation invariance, the  $(i+j)$ th order central moment is defined by:

$$\eta_{ij}^f = \iint_{\Omega} (x - \bar{x})^i (y - \bar{y})^j f(x, y) dx dy \quad (11)$$

where  $\bar{x} = \frac{\mu_{10}^f}{\mu_{00}^f}$  and  $\bar{y} = \frac{\mu_{01}^f}{\mu_{00}^f}$ .

Geometric moment invariants for the action of 2D transformation group  $G$  can be expressed as the functions of central moments. Suppose  $f(x, y)$  is transformed to  $h(u, v)$  using  $g \in G$ .  $GMI$  is a geometric moment invariant iff:

$$\begin{aligned} \forall g \in G : GMI(\eta_{00}^h, \eta_{10}^h, \eta_{01}^h, \eta_{20}^h, \eta_{11}^h, \eta_{02}^h, \dots) \\ = w(x, y; g) \cdot GMI(\eta_{00}^f, \eta_{10}^f, \eta_{01}^f, \eta_{20}^f, \eta_{11}^f, \eta_{02}^f, \dots) \end{aligned} \quad (12)$$

Similar to differential invariants defined in Sect.2.3, we suppose  $GMI$  is the homogeneous polynomial of central moments. The order and the degree of  $GMI$  are the maximum order of central moments it depends upon and the highest degree of individual terms in it. Also, polynomial geometric moment invariants can be used to construct non-polynomial ones.

Note that central moments and moment invariants detailed above are defined in the continuous domain. For the image function  $f(x, y) : \Omega \subset \mathbb{N}^+ \times \mathbb{N}^+ \rightarrow \mathbb{R}$ ,  $\mu_{ij}^f$  and  $\eta_{ij}^f$  are defined by:

$$\begin{aligned} \mu_{ij}^f &= \sum_{y=1}^{y=M} \sum_{x=1}^{x=N} x^i y^j f(x, y) \\ \eta_{ij}^f &= \sum_{y=1}^{y=M} \sum_{x=1}^{x=N} (x - \bar{x})^i (y - \bar{y})^j f(x, y) \end{aligned} \quad (13)$$

#### 2.5 Image Gaussian-Hermite Moment Invariants

Image Gaussian-Hermite moment invariants are a kind of orthogonal moment invariants. For the continuous function  $f(x, y) : \Omega \subset \mathbb{R} \times \mathbb{R} \rightarrow \mathbb{R}$ , the  $(i+j)$ th order Gaussian-Hermite moment is defined by:

$$\xi_{ij}^f = \iint_{\Omega} \hat{H}_i(x - \bar{x}; \sigma) \hat{H}_j(y - \bar{y}; \sigma) f(x, y) dx dy \quad (14)$$

The Gaussian-Hermite polynomial  $\hat{H}_i(x; \sigma)$  is defined by:

$$\begin{aligned} \hat{H}_i(x; \sigma) &= \frac{1}{(2^i i! \sqrt{\pi} \sigma)^{1/2}} e^{-\frac{x^2}{2\sigma^2}} H_i\left(\frac{x}{\sigma}\right) \\ H_i(x) &= (-1)^i e^{x^2} \frac{d^i e^{-x^2}}{dx^i} = \sum_{k=0}^{\lfloor \frac{i}{2} \rfloor} \frac{(-1)^{i-k} i!}{k! (i-2k)!} (2x)^{i-2k} \\ \bar{x} &= \frac{\mu_{10}^f}{\mu_{00}^f} \quad \text{and} \quad \bar{y} = \frac{\mu_{01}^f}{\mu_{00}^f} \end{aligned} \quad (15)$$

In this paper, the definition of Gaussian-Hermite moment invariants  $GHMI$  is similar to that of geometric moment invariants. The only difference between them is that  $GHMI$  are homogeneous polynomials of Gaussian-Hermite moments. When the domain  $\Omega \subset \mathbb{N}^+ \times \mathbb{N}^+$ ,  $\xi_{ij}^f$  is defined by:

$$\xi_{ij}^f = \sum_{y=1}^{y=M} \sum_{x=1}^{x=N} \hat{H}_i(x - \bar{x}; \sigma) \hat{H}_j(y - \bar{y}; \sigma) f(x, y) \quad (16)$$

#### 2.6 Independent Set of Image Differential Invariants

In this paper, we discuss three independent sets of image differential invariants, including linearly independent set, irreducible set and functional independent set.

Let  $S = \{DI_1, DI_2, \dots, DI_N\}$  be a set of differential invariants for the action of the transformation group  $G$ . Suppose the order of each invariant in  $S$  is less than or equal to  $M$ . This means that  $DI_i$  is the homogeneous polynomial of  $\frac{M(M+3)}{2}$  partial derivatives, where  $i \in \{1, 2, \dots, N\}$ .

$S$  is a linearly independent set iff:

$$\sum_{i=1}^{i=N} a_i DI_i = 0 \Leftrightarrow a_1 = a_2 = \dots = a_N = 0 \quad (17)$$

$S$  is an irreducible set iff:

$$\begin{aligned} \forall DI_i \in S, \nexists P \Rightarrow \\ DI_i = P(DI_1, DI_2, \dots, DI_{i-1}, DI_{i+1}, \dots, DI_N) \end{aligned} \quad (18)$$

where  $P$  is a polynomial function of differential invariants. Therefore, arbitrary differential invariants in the irreducible set  $S$  can not be express as the polynomial of other invariants.

If  $N \leq \frac{M(M+3)}{2}$ ,  $S$  is a functional independent set iff the rank of Jaccobian matrix  $N \times \frac{M(M+3)}{2}$  is equal to  $N$ .  $Jac$  is defined by:

$$Jac = \begin{vmatrix} \frac{\partial DI_1}{\partial f_{10}} & \frac{\partial DI_1}{\partial f_{01}} & \dots & \frac{\partial DI_1}{\partial f_{1(N-1)}} & \frac{\partial DI_1}{\partial f_{0N}} \\ \frac{\partial DI_2}{\partial f_{10}} & \frac{\partial DI_2}{\partial f_{01}} & \dots & \frac{\partial DI_2}{\partial f_{1(N-1)}} & \frac{\partial DI_2}{\partial f_{0N}} \\ \vdots & \vdots & \dots & \vdots & \vdots \\ \frac{\partial DI_{N-1}}{\partial f_{10}} & \frac{\partial DI_{N-1}}{\partial f_{01}} & \dots & \frac{\partial DI_{N-1}}{\partial f_{1(N-1)}} & \frac{\partial DI_{N-1}}{\partial f_{0N}} \\ \frac{\partial DI_N}{\partial f_{10}} & \frac{\partial DI_N}{\partial f_{01}} & \dots & \frac{\partial DI_N}{\partial f_{1(N-1)}} & \frac{\partial DI_N}{\partial f_{0N}} \end{vmatrix} \quad (19)$$

where  $f_{ij} = \frac{\partial^{i+j} f}{\partial x^i \partial y^j}$ ,  $i, j \in \{0, 1, 2, \dots\}$  and  $1 \leq (i + j) \leq N$ . This definition of functional independence was proposed by Brown (1935). Recently, Gong and Hao et al. (2017) use it to derive the functional independent set of shape-color moment invariants under affine transform.

### 3 Related Work

In this section, we first introduce some image differential invariants in explicit forms and how they are applied in the field of computer vision and pattern recognition. Then, currently commonly used methods to generate image differential invariants and geometric moments invariants are described. As mentioned previously, Li et al. (2017) proposed the isomorphism between differential invariants and geometric moment invariants under affine transform. We will introduce this discovery at the end of this section.

#### 3.1 Commonly Used Image Differential Invariants

In Table. 1, we list five differential invariants which have been widely used for image matching, classification and retrieval (Schmid and Mohr 1997; Mikolajczyk and Schmid 2005; Florack and Balmashnova 2008). Note that they are all homogeneous polynomials of image partial derivatives.  $DI_1 \sim DI_5$  are absolute Euclidean differential invariants and relative similarity differential invariants.  $DI_3$  and  $DI_4$  are relative invariant for the action of affine transformation group (Olver et al. 1999). Recently, Li and Mo et al. (2018) found  $DI_4$  is also a relative projective differential invariant.

There are different geometric meanings for these differential invariants. The Hessian matrix is built with second order partial derivatives of the image function  $f(x, y)$  and can be used to describe the local structure

Table 1: Five commonly used differential invariants.

No	Expression
$DI_1$	$(\frac{\partial f}{\partial x})^2 + (\frac{\partial f}{\partial y})^2$
$DI_2$	$\frac{\partial^2 f}{\partial x^2} + \frac{\partial^2 f}{\partial y^2}$
$DI_3$	$\frac{\partial^2 f}{\partial x^2} \frac{\partial^2 f}{\partial y^2} - (\frac{\partial^2 f}{\partial x \partial y})^2$
$DI_4$	$(\frac{\partial f}{\partial x})^2 \frac{\partial^2 f}{\partial y^2} - 2 \frac{\partial f}{\partial x} \frac{\partial f}{\partial y} \frac{\partial^2 f}{\partial x \partial y} + (\frac{\partial f}{\partial y})^2 \frac{\partial^2 f}{\partial x^2}$
$DI_5$	$(\frac{\partial f}{\partial y})^2 \frac{\partial^2 f}{\partial x \partial y} + \frac{\partial f}{\partial x} \frac{\partial f}{\partial y} \frac{\partial^2 f}{\partial x^2} - \frac{\partial f}{\partial x} \frac{\partial f}{\partial y} \frac{\partial^2 f}{\partial y^2} -$ $(\frac{\partial f}{\partial x})^2 \frac{\partial^2 f}{\partial x \partial y}$

of  $f(x, y)$  in the neighborhood of the point  $(x_0, y_0)$ . It is defined as:

$$H(x_0, y_0; \sigma) = \begin{pmatrix} L_{20}(x_0, y_0; \sigma) & L_{11}(x_0, y_0; \sigma) \\ L_{11}(x_0, y_0; \sigma) & L_{02}(x_0, y_0; \sigma) \end{pmatrix} \quad (20)$$

As stated in Sect.2.2,  $L_{ij}(x_0, y_0; \sigma)$  is used to estimate the value of  $\frac{\partial^{i+j} f}{\partial x^i \partial y^j}$ . Thus, the determinant and the trace of the Hessian matrix are  $DI_2$  and  $DI_3$ . Researchers have found  $DI_2$  can be used to detect blob structures or determine the characteristic scale for every interest point in the image (Lindeberg 1994; Lindeberg and Gårding 1997; Mikolajczyk and Schmid 2001; Mikolajczyk and Schmid 2004; Mikolajczyk et al.2005). In addition, two eigenvalues of this matrix are:

$$\lambda_1 = \frac{1}{2} \left( \frac{\partial^2 f}{\partial x^2} + \frac{\partial^2 f}{\partial y^2} + \sqrt{\left( \frac{\partial^2 f}{\partial x^2} - \frac{\partial^2 f}{\partial y^2} \right)^2 + \left( \frac{\partial^2 f}{\partial x \partial y} \right)^2} \right)$$

$$\lambda_2 = \frac{1}{2} \left( \frac{\partial^2 f}{\partial x^2} + \frac{\partial^2 f}{\partial y^2} - \sqrt{\left( \frac{\partial^2 f}{\partial x^2} - \frac{\partial^2 f}{\partial y^2} \right)^2 + \left( \frac{\partial^2 f}{\partial x \partial y} \right)^2} \right) \quad (21)$$

We can find  $\lambda_1 = \frac{1}{2}(DI_2 + \sqrt{(DI_2)^2 - 4DI_3})$  and  $\lambda_2 = \frac{1}{2}(DI_2 - \sqrt{(DI_2)^2 - 4DI_3})$ . Thus, they are two non-polynomial differential invariants which can be expressed as the functions of homogeneous polynomial ones.

In the classical theory of differential geometry, there are two important concepts on the curved surface  $f(x, y)$ , the Gaussian curvature  $K(x, y)$  and the mean curvature  $H(x, y)$ :

$$K(x, y) = \frac{\frac{\partial^2 f}{\partial x^2} \frac{\partial^2 f}{\partial y^2} - \left( \frac{\partial^2 f}{\partial x \partial y} \right)^2}{\left( 1 + \left( \frac{\partial f}{\partial x} \right)^2 + \left( \frac{\partial f}{\partial y} \right)^2 \right)^2}$$

$$H(x, y) = \frac{\left( 1 + \left( \frac{\partial f}{\partial y} \right)^2 \right) \frac{\partial^2 f}{\partial x^2} - 2 \frac{\partial f}{\partial x} \frac{\partial f}{\partial y} \frac{\partial^2 f}{\partial x \partial y} + \left( 1 + \left( \frac{\partial f}{\partial x} \right)^2 \right) \frac{\partial^2 f}{\partial y^2}}{2 \left( 1 + \left( \frac{\partial f}{\partial x} \right)^2 + \left( \frac{\partial f}{\partial y} \right)^2 \right)^{\frac{3}{2}}} \quad (22)$$

They are invariant under 2D Euclidean transform. In fact,  $K(x, y) = \frac{DI_3}{(1+DI_1)^2}$  and  $H(x, y) = \frac{DI_2+DI_4}{2(1+DI_1)^{\frac{3}{2}}}$ . In addition, at a given point of the surface  $f(x, y)$ , two

principal curvatures are defined by  $\kappa_1 = H + \sqrt{H^2 - K}$  and  $\kappa_2 = H - \sqrt{H^2 - K}$ . Based on them, Koenderink and van Doorn (1992) constructed the shape index  $s$  and the curvedness  $c$  to measure the image local shape:

$$\begin{aligned} s &= \frac{2}{\pi} \operatorname{actan} \frac{\kappa_2 - \kappa_1}{\kappa_2 + \kappa_1} \\ &= \frac{2}{\pi} \operatorname{actan} \frac{-(DI_2 + DI_4)}{\sqrt{(DI_2 + DI_4)^2 - 4(1 + DI_1)DI_3}} \\ c &= \sqrt{\frac{\kappa_1^2 + \kappa_2^2}{2}} = \sqrt{\frac{(DI_2 + DI_4)^2 - 2DI_3(1 + DI_1)}{2(1 + DI_1)^3}} \end{aligned} \quad (23)$$

In 1993, Freeman and Adelson (1990) designed steerable filters to calculate directional derivatives of the image function  $f(x, y)$ . The first and second directional derivatives at an arbitrary orientation  $\theta$  are defined by:

$$\begin{aligned} f^1(\theta) &= \cos \theta \frac{\partial f}{\partial x} + \sin \theta \frac{\partial f}{\partial y} \\ f^2(\theta) &= \cos^2 \theta \frac{\partial^2 f}{\partial x^2} + 2 \sin \theta \cos \theta \frac{\partial^2 f}{\partial x \partial y} + \sin^2 \theta \frac{\partial^2 f}{\partial y^2} \end{aligned} \quad (24)$$

Zhang et al. (2013) have found that the minimum and maximum values of  $f^1(\theta)$  and  $f^2(\theta)$  are invariant under 2D Euclidean transform:

$$f_{min}^1 = 0, f_{max}^1 = DI_1, f_{max}^2 = \lambda_1, f_{min}^2 = \lambda_2 \quad (25)$$

where  $\lambda_1$  and  $\lambda_2$  are defined by Eq.(21). Therefore, they are also the functions of invariants in Table. 1. Researchers have constructed many effective local descriptors based on these non-polynomial differential invariants for image matching and texture classification (Song et al.2017; Song et al.2018; Zhang et al.2013).

In the past ten years, Griffin have published many papers concerned with the analysis of image local structure. In 2007, he proposed the norm of local jet of order 2 (Griffin 2007; Griffin 2019). The local jet has been defined by Eq.(7). This norm was invariant under 2D Euclidean transform and defined by:

$$\begin{aligned} \|J^2(x_0, y_0; \sigma)\| &= ((L_{10}^2(x_0, y_0; \sigma) + L_{01}^2(x_0, y_0; \sigma)) \\ &\quad + \frac{1}{2}(L_{20}^2(x_0, y_0; \sigma) + 2L_{11}^2(x_0, y_0; \sigma) \\ &\quad + L_{02}^2(x_0, y_0; \sigma)))^{\frac{1}{2}} \end{aligned} \quad (26)$$

We find it can be expressed as:

$$\sqrt{DI_1 + \frac{1}{4}DI_2^2 + \frac{1}{4}(DI_2^2 - 4DI_3)} \quad (27)$$

Then, Griffin and Lillholm (2010) studied the relation between the value of  $J^2(x_0, y_0; \sigma)$  and the symmetry of the image  $f(x, y)$  in the neighborhood of the point  $(x_0, y_0)$ . In Sect.2.3, we have pointed out that image partial derivatives can not be used to describe intrinsic property of  $f(x, y)$ , such as symmetry. In order to solve this problem, they proposed a new coordinate system  $(l, b, a)$  based on the norm defined by Eq.(26). We find that  $l$ ,  $b$  and  $a$  are all non-polynomial differential invariants for the action of 2D Euclidean transformation group and can be formed by:

$$\begin{aligned} l &= \operatorname{actan} \frac{DI_2}{\sqrt{4DI_1 + DI_2^2 - 4DI_3}} \\ b &= \operatorname{actan} \sqrt{\frac{DI_2^2 - 4DI_3}{4DI_1}} \\ a &= \frac{1}{2} \left| \operatorname{actan} \frac{2DI_5}{DI_1DI_2 - 2DI_4} \right| \end{aligned} \quad (28)$$

In 2010, Crosier and Griffin (2019) proposed the Basic Images Feature(BIF) for texture classification:

$$\begin{aligned} BIF &= (2\sqrt{L_{10}^2(x_0, y_0; \sigma) + L_{01}^2(x_0, y_0; \sigma)} \\ &\quad \pm (L_{20}(x_0, y_0; \sigma) + L_{02}(x_0, y_0; \sigma)), \\ &\quad \frac{1}{\sqrt{2}}(\sqrt{(L_{20}(x_0, y_0; \sigma) - L_{02}(x_0, y_0; \sigma))^2 + 4L_{11}^2(x_0, y_0; \sigma)} \\ &\quad \pm (L_{20}(x_0, y_0; \sigma) + L_{02}(x_0, y_0; \sigma))), \\ &\quad \sqrt{(L_{20}(x_0, y_0; \sigma) - L_{02}(x_0, y_0; \sigma))^2 + 4L_{11}^2(x_0, y_0; \sigma)}) \end{aligned} \quad (29)$$

We can express BIF as:

$$\begin{aligned} BIF &= (2\sqrt{DI_1}, \pm(DI_2), \frac{1}{\sqrt{2}}(\sqrt{DI_2^2 - 4DI_3} \pm DI_2), \\ &\quad \sqrt{DI_2^2 - 4DI_3}) \end{aligned} \quad (30)$$

In fact, this 6-dimensional vector includes image gradient magnitude, Laplacian, two eigenvalues of the Hessian matrix and the difference between them.

There are many other applications for  $DI_1 \sim DI_5$ . For example, the curvature of a level curve multiplied by the gradient magnitude can be expressed as  $\frac{-DI_4}{DI_1}$ .  $DI_4$  can be used to detect corners in the image  $f(x, y)$  because it corresponds to the second derivative in the direction orthogonal to the gradient of  $f(x, y)$ .

### 3.2 Commonly Used Methods of Generating Image Differential Invariants

We can find that the order of arbitrary invariants in Table. 1 is less than or equal to 2. This is because higher

order differential invariants are hard to be generated. Also, assigning proper geometrical meanings to them is a problem.

In the past researchers commonly used the method of moving frame to derive higher order differential invariants for the action of various transformation groups. Cartan formulated the general definition of the method of moving frame, as elaborated by Wely. But this method was difficult and complicated. To address this problem, Olver have published many papers and books to explain how to use the method of moving frame more simply and straightforwardly. For example, he proposed that a complete system of image differential invariants for the action of 2D equi-affine group was provided by its invariant derivatives obtained by repeatedly applying the invariant differential operators  $\mathcal{D}_1$  and  $\mathcal{D}_2$  (Olver 2015). The 2D equi-affine transformation  $g$  is defined by Eq.(3), where  $(ac - bd) = 1$ .  $\mathcal{D}_1$  and  $\mathcal{D}_2$  was defined by:

$$\begin{aligned}\mathcal{D}_1 &= \frac{\partial f}{\partial y} \mathcal{D}_x - \frac{\partial f}{\partial x} \mathcal{D}_y \\ \mathcal{D}_2 &= \left( \frac{\partial f}{\partial x} \frac{\partial^2 f}{\partial y^2} - \frac{\partial f}{\partial y} \frac{\partial^2 f}{\partial x \partial y} \right) \mathcal{D}_x \\ &\quad + \left( \frac{\partial f}{\partial y} \frac{\partial^2 f}{\partial x^2} - \frac{\partial f}{\partial x} \frac{\partial^2 f}{\partial x \partial y} \right) \mathcal{D}_y\end{aligned}\quad (31)$$

However, we find that all image differential invariants generated by repeatedly applying  $\mathcal{D}_1$  and  $\mathcal{D}_2$  depend upon the first partial derivatives, such as:

$$\begin{aligned}(\mathcal{D}_2, f) &= \left( \frac{\partial f}{\partial x} \right)^2 \frac{\partial^2 f}{\partial y^2} - 2 \frac{\partial f}{\partial x} \frac{\partial f}{\partial y} \frac{\partial^2 f}{\partial x \partial y} + \left( \frac{\partial f}{\partial y} \right)^2 \frac{\partial^2 f}{\partial x^2} \\ (\mathcal{D}_1 \circ \mathcal{D}_2, f) &= \left( \frac{\partial f}{\partial y} \right)^3 \frac{\partial^3 f}{\partial x^3} + 3 \left( \frac{\partial f}{\partial x} \right)^2 \frac{\partial f}{\partial y} \frac{\partial^3 f}{\partial x \partial y^2} \\ &\quad - 3 \frac{\partial f}{\partial x} \left( \frac{\partial f}{\partial y} \right)^2 \frac{\partial^3 f}{\partial x^2 \partial y} - \left( \frac{\partial f}{\partial x} \right)^3 \frac{\partial^3 f}{\partial y^3}\end{aligned}\quad (32)$$

where  $\circ$  denotes the composition of differential operators. The derivation of differential invariants which are independent of the first partial derivatives is very complicated. For example,  $DI_3$  in Table. 1 is obtained by:

$$DI_3 = \frac{(\mathcal{D}_1 \circ \mathcal{D}_2 \circ \mathcal{D}_2, f) - (\mathcal{D}_2 \circ \mathcal{D}_1 \circ \mathcal{D}_2, f)}{2(\mathcal{D}_1 \circ \mathcal{D}_2, f)} \quad (33)$$

Florack et al. (1993) proposed a irreducible set of image Euclidean differential invariants consisted of the directional derivatives along the gradient direction  $w$  and the direction  $v$  orthogonal to the gradient of the image function  $f(x, y)$ . These directional derivatives were

defined by:

$$\begin{aligned}\frac{\partial f}{\partial v} &= -\beta \frac{\partial f}{\partial x} + \alpha \frac{\partial f}{\partial y} \\ \frac{\partial f}{\partial w} &= \alpha \frac{\partial f}{\partial x} + \beta \frac{\partial f}{\partial y} \\ \frac{\partial^2 f}{\partial v^2} &= -\beta \left( -\beta \frac{\partial^2 f}{\partial x^2} + \alpha \frac{\partial^2 f}{\partial x \partial y} \right) + \alpha \left( -\beta \frac{\partial^2 f}{\partial x \partial y} + \alpha \frac{\partial^2 f}{\partial y^2} \right) \\ \frac{\partial^2 f}{\partial v \partial w} &= -\beta \left( \alpha \frac{\partial^2 f}{\partial x^2} + \beta \frac{\partial^2 f}{\partial x \partial y} \right) + \alpha \left( \alpha \frac{\partial^2 f}{\partial x \partial y} + \beta \frac{\partial^2 f}{\partial y^2} \right) \\ &\vdots\end{aligned}\quad (34)$$

where  $\alpha = \frac{\frac{\partial f}{\partial x}}{\sqrt{(\frac{\partial f}{\partial x})^2 + (\frac{\partial f}{\partial y})^2}}$  and  $\beta = \frac{\frac{\partial f}{\partial y}}{\sqrt{(\frac{\partial f}{\partial x})^2 + (\frac{\partial f}{\partial y})^2}}$ .

Using this method, Ter Haar Romeny et al. (1994) derived the irreducible set when setting the order of differential invariants to be less than or equal to 4:

$$\left\{ \frac{\partial^{i+j} f}{\partial v^i \partial w^j} \left( \frac{\partial f}{\partial w} \right)^{i+j} \right\}_{i,j \in \{0,1,2,3,4\}, 0 < (i+j) \leq 4} \quad (35)$$

But similar to Olver's method, all differential invariants in this set depend upon the first partial derivatives, such as:

$$\begin{aligned}\frac{\partial^2 f}{\partial w^2} \left( \frac{\partial f}{\partial w} \right)^2 &= \left( \frac{\partial f}{\partial x} \right)^2 \frac{\partial^2 f}{\partial x^2} + 2 \frac{\partial f}{\partial x} \frac{\partial f}{\partial y} \frac{\partial^2 f}{\partial x \partial y} + \left( \frac{\partial f}{\partial y} \right)^2 \frac{\partial^2 f}{\partial y^2} \\ \frac{\partial^2 f}{\partial w^3} \left( \frac{\partial f}{\partial w} \right)^3 &= \left( \frac{\partial f}{\partial x} \right)^3 \frac{\partial^3 f}{\partial x^3} + 3 \left( \frac{\partial f}{\partial x} \right)^2 \frac{\partial f}{\partial y} \frac{\partial^3 f}{\partial x^2 \partial y} \\ &\quad + 3 \frac{\partial f}{\partial x} \left( \frac{\partial f}{\partial y} \right)^2 \frac{\partial^3 f}{\partial x \partial y^2} + \left( \frac{\partial f}{\partial y} \right)^3 \frac{\partial^3 f}{\partial y^3}\end{aligned}\quad (36)$$

To summarize, it is hard to generate a large number of differential invariants with general forms using these existing methods. In this paper, we report a new method which can overcome these limitations.

### 3.3 Two Generating Functions for Geometric Moment Invariants

As mentioned previously, researchers have designed many intuitive methods to generate image moment invariants. Li et al. (2017) proposed that image geometric moment invariants can be derived using dot product and cross product of 2D points.

Suppose the image function  $f(x, y) : \Omega \subset \mathbb{N}^+ \times \mathbb{N}^+ \rightarrow \mathbb{R}$  is transformed to  $h(u, v) : \Omega' \subset \mathbb{N}^+ \times \mathbb{N}^+ \rightarrow \mathbb{R}$  using the 2D transformation  $g$ . Let  $(u_i, v_i)$  and  $(u_j, v_j) \in \Omega'$  be corresponding points of  $(x_i, y_i)$  and  $(x_j, y_j) \in \Omega$ .

The dot product and cross product of 2D points are defined as:

$$\begin{aligned} f_{i,j} &= (x_i - \bar{x}, y_i - \bar{y}) \cdot (x_j - \bar{x}, y_j - \bar{y})^T = \\ &= (x_i - \bar{x}) \cdot (x_j - \bar{x}) + (y_i - \bar{y})(y_j - \bar{y}) \\ g_{i,j} &= \begin{vmatrix} x_i - \bar{x} & y_i - \bar{y} \\ x_j - \bar{x} & y_j - \bar{y} \end{vmatrix} \\ &= (x_i - \bar{x}) \cdot (y_j - \bar{y}) - (x_j - \bar{x})(y_i - \bar{y}) \end{aligned} \quad (37)$$

Note that  $\bar{x} = \frac{\mu_{10}^f}{\mu_{00}^f}$  and  $\bar{y} = \frac{\mu_{01}^f}{\mu_{00}^f}$ . As stated in Sect.(2.4), they are used to remove the effect of translation.

The relations between  $f_{i,j}$  ( $g_{i,j}$ ) and  $f'_{i,j}$  ( $g'_{i,j}$ ) are listed in Table. 2, where  $f'_{i,j}$  and  $g'_{i,j}$  denote the dot product and the cross product of  $(u_i, v_i)$  and  $(u_j, v_j)$ . Based on them, geometric moment invariants of the image function  $f(x, y)$  can be generated by:

$$\begin{aligned} GMI(f) &= \sum_{y_n=1}^{y_n=M} \sum_{x_n=1}^{x_n=N} \dots \sum_{y_1=1}^{y_1=M} \sum_{x_1=1}^{x_1=N} \prod_{p=1}^{p=P} f_{i_p, j_p} \\ &\cdot \prod_{q=1}^{q=Q} g_{s_q, t_q} \cdot \prod_{k=1}^{k=n} f(x_k, y_k) \end{aligned} \quad (38)$$

where  $(x_1, y_1), (x_2, y_2), \dots, (x_k, y_k), \dots, (x_n, y_n) \in \Omega$  and  $i_p, j_p, s_q, t_q \in \{1, 2, \dots, n\}$ . Each point  $(x_k, y_k)$  is used at least once by  $f_{i_p, j_p}$  or  $g_{s_q, t_q}$  in Eq.(38).

$GMI(f)$  is an absolute moment invariant when  $g$  belongs to 2D Euclidean transformation group. If  $g$  is a 2D similarity transformation,  $GMI(h) = (s^2)^{P+Q+n} \cdot GMI(f)$ . When  $P = 0$ , which implies only the cross product  $g_{s_q, t_q}$  is used, Eq.(38) generates an affine moment invariant. We can find that  $GMI(h) = (ad - bc)^Q |ad - bc|^n GMI(f)$ .

$GMI(f)$  can be expressed as the homogeneous polynomial of central moments defined by Eq.(13). For example,

$$\begin{aligned} GMI(f) &= \sum_{y_1=1}^{y_1=M} \sum_{x_1=1}^{x_1=N} f_{1,1} f(x_1, y_1) \\ &= \sum_{y_1=1}^{y_1=M} \sum_{x_1=1}^{x_1=N} ((x_1 - \bar{x})^2 + (y_1 - \bar{y})^2) f(x_1, y_1) \\ &= \eta_{20}^f + \eta_{02}^f \end{aligned} \quad (39)$$

Thus,  $GMI(f)$  meets the definition of geometric moment invariants in Sect.2.4. The degree of the moment invariant defined by Eq.(38) is  $n$ . If  $T(x_k, y_k)$  denotes the number of times that  $(x_k, y_k)$  is used by  $f_{i_p, j_p}$  and  $g_{s_q, t_q}$ , the order of  $GMI(f)$  is  $\max_k T(x_k, y_k)$ . It is equal to the maximum order of central moments that  $GMI(f)$  depends upon.

The fundamental generating functions can also be extended to generate 3D moment invariants of the function  $f(x, y, z) : \Omega \subset \mathbb{N}^+ \times \mathbb{N}^+ \times \mathbb{N}^+ \rightarrow \mathbb{R}$ :

$$\begin{aligned} f_{i,j} &= (x_i - \bar{x}, y_i - \bar{y}, z_i - \bar{z}) \cdot (x_j - \bar{x}, y_j - \bar{y}, z_j - \bar{z})^T \\ g_{i,j,k} &= \begin{vmatrix} x_i - \bar{x} & y_i - \bar{y} & z_i - \bar{z} \\ x_j - \bar{x} & y_j - \bar{y} & z_j - \bar{z} \\ x_k - \bar{x} & y_k - \bar{y} & z_k - \bar{z} \end{vmatrix} \end{aligned} \quad (40)$$

where  $(x_i, y_i, z_i), (x_j, y_j, z_j), (x_k, y_k, z_k) \in \Omega$ .  $\bar{x}, \bar{y}$  and  $\bar{z}$  are calculated by using 3D central moments, for example,  $\bar{x} = \frac{\mu_{100}^f}{\mu_{000}^f}$ .

### 3.4 Isomorphism between Affine Differential and Geometric Moment Invariants

Li et al. (2017) have found that affine differential invariants of the image function  $f(x, y)$  can be derived by substituting central moment  $\eta_{ij}^f$  in affine geometric moment invariants by image partial derivatives  $\frac{\partial^{i+j} f}{\partial x^i \partial y^j}$ .

Actually, under 2D affine transform, the steerability of  $n$  order partial derivatives is the same as that of  $n$  order central moments. Li et al. called this property isomorphism between affine differential and moment invariants. For example, if the image function  $f(x, y)$  is transformed to  $h(u, v)$  using the 2D affine transformation  $g$  defined by Eq.(3), we have:

$$\begin{aligned} \begin{pmatrix} \eta_{20}^h \\ \eta_{11}^h \\ \eta_{02}^h \end{pmatrix} &= \begin{pmatrix} a^2 & 2ab & b^2 \\ ac & (ad+bc) & bd \\ c^2 & 2cd & d^2 \end{pmatrix} \begin{pmatrix} \eta_{20}^f \\ \eta_{11}^f \\ \eta_{02}^f \end{pmatrix} \\ \begin{pmatrix} \frac{\partial^2 h}{\partial u^2} \\ \frac{\partial^2 h}{\partial u \partial v} \\ \frac{\partial^2 h}{\partial v^2} \end{pmatrix} &= \begin{pmatrix} (a')^2 & 2a'b' & (b')^2 \\ a'c' & (a'd' + b'c') & b'd' \\ (c')^2 & 2c'd' & (d')^2 \end{pmatrix} \begin{pmatrix} \frac{\partial^2 f}{\partial x^2} \\ \frac{\partial^2 f}{\partial x \partial y} \\ \frac{\partial^2 f}{\partial y^2} \end{pmatrix} \end{aligned} \quad (41)$$

where

$$\begin{pmatrix} a' & b' \\ c' & d' \end{pmatrix} = \left( \begin{pmatrix} a & b \\ c & d \end{pmatrix}^{-1} \right)^T = g' \quad (42)$$

Obviously,  $g'$  is also a 2D affine transformation. Therefore, we have:

$$\begin{aligned} GMI(h, \frac{\partial h}{\partial u}, \frac{\partial h}{\partial v}, \frac{\partial^2 h}{\partial u^2}, \frac{\partial^2 h}{\partial u \partial v}, \frac{\partial^2 h}{\partial v^2}, \dots) \\ = w(x, y, g') \cdot GMI(f, \frac{\partial f}{\partial x}, \frac{\partial f}{\partial y}, \frac{\partial^2 f}{\partial x^2}, \frac{\partial^2 f}{\partial x \partial y}, \frac{\partial^2 f}{\partial y^2}, \dots) \end{aligned}$$



Table 2: The relations between  $f_{i,j}$  ( $g_{i,j}$ ) and  $f'_{i,j}$  ( $g'_{i,j}$ ) when  $g$  belongs to various transformation groups.

$g$	Relation	Relation
2D Euclidean Transformation (Defined by Eq.(1))	$f'_{i,j} = f_{i,j}$	$g'_{i,j} = g_{i,j}$
2D Similarity Transformation (Defined by Eq.(2))	$f'_{i,j} = s^2 \cdot f_{i,j}$	$g'_{i,j} = s^2 \cdot g_{i,j}$
2D Affine Transformation (Defined by Eq.(3))	/	$g'_{i,j} = (ad - bc) \cdot g_{i,j}$

(43)  $F_{i,j}$  and  $G_{i,j}$  are defined by:

when:

$$\begin{aligned} & GMI(\eta_{00}^h, \eta_{10}^h, \eta_{01}^h, \eta_{20}^h, \eta_{11}^h, \eta_{02}^h \dots) \\ & = w(x, y, g) \cdot GMI(\eta_{00}^f, \eta_{10}^f, \eta_{01}^f, \eta_{20}^f, \eta_{11}^f, \eta_{02}^f \dots) \end{aligned} \quad (44)$$

Although Li et al. found the relation between image differential invariants and geometric moment invariants under 2D affine transform, the proof in their paper was informal and imprecise.

#### 4 A New Construction Method of Image Differential Invariants

Inspired by Li's discovery introduced in Sect.3.4 and the methods of systematic derivation of geometric moment invariants, we find that two fundamental differential operators can be employed to systematically generate image Euclidean, similarity and affine differential invariants. When setting the order and the degree to be less than or equal to 4, all Euclidean differential invariants are generated by using the new method. Then, we discuss the independence of them and obtain the linearly independent set, irreducible set and functional independent set. Although we don't find the general method to generate differential invariants for the action of more complicated transformation groups, some projective and conformal differential invariants are found from Euclidean ones. Finally, our method can also be extended to generate 3D differential invariants.

##### 4.1 Two Fundamental Differential Operators

Similar to two generating functions of geometric moment invariants introduced in Sect.3.3, we get the following definition.

**Definition 1.** Two fundamental differential operators

$$\begin{aligned} F_{i,j} &= \frac{\partial^2}{\partial x_i \partial x_j} + \frac{\partial^2}{\partial y_i \partial y_j} \\ G_{i,j} &= \left| \begin{array}{cc} \frac{\partial}{\partial x_i} & \frac{\partial}{\partial y_i} \\ \frac{\partial}{\partial x_j} & \frac{\partial}{\partial y_j} \end{array} \right| = \frac{\partial^2}{\partial x_i \partial y_j} - \frac{\partial^2}{\partial x_j \partial y_i} \end{aligned} \quad (45)$$

We find that they are absolute or relative invariant under 2D Euclidean, similarity and affine transforms.

**Theorem 1.** Suppose  $(x_i, y_i)$  and  $(x_j, y_j)$  are transformed to  $(u_i, v_i)$  and  $(u_j, v_j)$  using the 2D transformation  $g$ . The relations between  $F_{i,j}$  ( $G_{i,j}$ ) and  $F'_{i,j}$  ( $G'_{i,j}$ ) are listed in Table. 3, when  $g$  belongs to various 2D transformation groups. The differential operators  $F'_{i,j}$  and  $G'_{i,j}$  are obtained by replacing  $x_k$  and  $y_k$  in Eq.(45) with  $u_k$  and  $v_k$ , where  $k \in \{i, j\}$ .

Theorem 1 can be proved by using the chain's rule for the compound function. For example, when  $g$  is the 2D affine transformation defined by Eq.(3), we can get its inverse transformation:

$$\begin{aligned} x_k(u_k, v_k) &= \frac{du_k - bv_k}{ad - bc} + \frac{bt_2 - dt_1}{ad - bc} \\ y_k(u_k, v_k) &= \frac{av_k - cu_k}{ad - bc} + \frac{ct_1 - at_2}{ad - bc} \end{aligned} \quad (46)$$

where  $k \in \{i, j\}$ . Then, according to the chain's rule, we can find:

$$\begin{aligned} G'_{i,j} &= \frac{\partial^2}{\partial u_i \partial v_j} - \frac{\partial^2}{\partial u_j \partial v_i} = \left( \frac{\partial^2}{\partial x_i \partial x_j} \frac{\partial x_i}{\partial u_i} \frac{\partial x_j}{\partial v_j} \right. \\ &+ \frac{\partial^2}{\partial x_i \partial y_j} \frac{\partial x_i}{\partial u_i} \frac{\partial y_j}{\partial v_j} + \frac{\partial^2}{\partial x_j \partial y_i} \frac{\partial x_j}{\partial v_j} \frac{\partial y_i}{\partial u_i} \\ &+ \left. \frac{\partial^2}{\partial y_i \partial y_j} \frac{\partial y_i}{\partial u_i} \frac{\partial y_j}{\partial v_j} \right) - \left( \frac{\partial^2}{\partial x_i \partial x_j} \frac{\partial x_i}{\partial v_i} \frac{\partial x_j}{\partial u_j} \right. \\ &+ \frac{\partial^2}{\partial x_j \partial y_i} \frac{\partial x_j}{\partial v_i} \frac{\partial y_i}{\partial u_j} + \frac{\partial^2}{\partial x_i \partial y_j} \frac{\partial x_i}{\partial v_j} \frac{\partial y_j}{\partial u_i} \\ &+ \left. \frac{\partial^2}{\partial y_i \partial y_j} \frac{\partial y_i}{\partial v_i} \frac{\partial y_j}{\partial u_j} \right) = \frac{1}{(ad - bc)} \cdot G_{i,j} \end{aligned} \quad (47)$$

It should be noted that  $\frac{\partial^2 x_k}{\partial u_k^2} = \frac{\partial^2 x_k}{\partial u_k \partial v_k} = \frac{\partial^2 x_k}{\partial v_k^2} = \frac{\partial^2 y_k}{\partial u_k^2} = \frac{\partial^2 y_k}{\partial u_k \partial v_k} = \frac{\partial^2 y_k}{\partial v_k^2} = 0$ .

Table 3: The relations between  $F_{i,j}$  ( $G_{i,j}$ ) and  $F'_{i,j}$  ( $G'_{i,j}$ ) when  $g$  belongs to various transformation groups.

$g$	Relation	Relation
2D Euclidean Transformation (Defined by Eq.(1))	$F'_{i,j} = F_{i,j}$	$G'_{i,j} = G_{i,j}$
2D Similarity Transformation (Defined by Eq.(2))	$F'_{i,j} = \frac{1}{s^2} \cdot F_{i,j}$	$G'_{i,j} = \frac{1}{s^2} \cdot G_{i,j}$
2D Affine Transformation (Defined by Eq.(3))	/	$G'_{i,j} = \frac{1}{(ad-bc)} \cdot G_{i,j}$

## 4.2 The Construction of Image Differential Invariants

(52)

Based on two fundamental differential operators defined by Eq.(45) and the relations listed in Table. 3, image differential invariants for the action of 2D Euclidean, similarity and affine transformation groups can be generated.

**Definition 2.** Suppose the image function  $f(x, y) : \Omega \subset \mathbb{N}^+ \times \mathbb{N}^+ \rightarrow \mathbb{R}$  has infinite order partial derivatives. Let  $(x_k, y_k) \in \Omega$  and  $k \in \{1, 2, \dots, n\}$ . We construct a function  $F$  by:

$$F = f(x_1, y_1) \cdot \dots \cdot f(x_k, y_k) \cdot \dots \cdot f(x_n, y_n) \quad (48)$$

Then, the differential invariant of  $F$  can be generated by:

$$DI(F) = (F_{i_P, j_P} \circ \dots \circ F_{i_p, j_p} \circ \dots \circ F_{i_1, j_1} \circ G_{s_Q, t_Q} \circ \dots \circ G_{s_q, t_q} \circ \dots \circ G_{s_1, t_1}, F) \quad (49)$$

where  $\circ$  denotes the composition of differential operators. Each point  $(x_k, y_k)$  is used at least once by  $F_{i_p, j_p}$  or  $G_{s_q, t_q}$  in Eq.(49).

**Theorem 2.** Suppose the image function  $f(x, y) : \Omega \subset \mathbb{N}^+ \times \mathbb{N}^+ \rightarrow \mathbb{R}$  has infinite order partial derivatives. We transform it to  $h(u, v) : \Omega' \subset \mathbb{N}^+ \times \mathbb{N}^+ \rightarrow \mathbb{R}$  using the 2D transformation  $g$ . Let  $(u_k, v_k) \in \Omega'$  be corresponding points of  $(x_k, y_k) \in \Omega$ , where  $k \in \{1, 2, \dots, n\}$ . We defined  $DI'(H)$  by:

$$DI'(H) = (F'_{i_P, j_P} \circ \dots \circ F'_{i_p, j_p} \circ \dots \circ F'_{i_1, j_1} \circ G'_{s_Q, t_Q} \circ \dots \circ G'_{s_q, t_q} \circ \dots \circ G'_{s_1, t_1}, H) \quad (50)$$

where

$$H = h(u_1, v_1) \cdot \dots \cdot h(u_k, v_k) \cdot \dots \cdot h(u_n, v_n) \quad (51)$$

Then, we have

$$DI'(H) = DI(F), \text{ when } g \text{ is defined by Eq.(1)}$$

$$DI'(H) = \frac{DI(F)}{s^{2(P+Q)}}, \text{ when } g \text{ is defined by Eq.(2)}$$

$$DI'(H) = \frac{DI(F)}{(ad-bc)^Q}, \text{ when } P=0 \text{ and } g \text{ is defined by Eq.(3)}$$

We can prove Theorem 2 by using the relations in Table. 3 and the linearity of fundamental differential operators  $F_{i,j}$  and  $G_{i,j}$ . Obviously,  $DI(F)$  is an absolute Euclidean differential invariant. Also, it is relative invariant under 2D similarity and affine transforms.

However, Eq.(49) generates differential invariants of the function  $F(x_1, \dots, x_n, y_1, \dots, y_n)$  instead of the image function  $f(x, y)$ . This problem can be solved easily. To solve this we first construct  $DI(F)$  and then set  $x_1=x_2=\dots=x_n=x$ ,  $y_1=y_2=\dots=y_n=y$ . For example,

$$\begin{aligned} DI(F) &= (G_{1,2} \circ G_{1,2}, f(x_1, y_1) \cdot f(x_2, y_2)) \\ &= G_{1,2}(G_{1,2}(f(x_1, y_1) \cdot f(x_2, y_2))) \\ &= \frac{\partial^2 f}{\partial x_1^2} \frac{\partial^2 f}{\partial y_2^2} - 2 \frac{\partial^2 f}{\partial x_1 \partial y_1} \frac{\partial^2 f}{\partial x_2 \partial y_2} + \frac{\partial^2 f}{\partial x_2^2} \frac{\partial^2 f}{\partial y_1^2} \end{aligned} \quad (53)$$

By setting  $x_1=x_2=x$  and  $y_1=y_2=y$ , we obtain the differential invariant of  $f(x, y)$ :

$$DI(f) = 2 \frac{\partial^2 f}{\partial x^2} \frac{\partial^2 f}{\partial y^2} - 2 \frac{\partial^2 f}{\partial x \partial y} \quad (54)$$

All image differential invariants constructed using Eq.(49) are homogeneous polynomials of image partial derivatives. As mentioned in Sect.2.3, researchers have proved that non-polynomial differential invariants can be expressed as the functions of these polynomial ones. The degree of  $DI(f)$  is equal to  $n$ , the number of points which are used by  $F_{i_p, j_p}$  and  $G_{s_q, t_q}$  in Eq.(49). Actually, we can find that  $n$  decides the highest degree of individual terms in  $DI(f)$ . The order of  $DI(f)$  is the most times that points are repeatedly used in Eq.(49). Its value is also equal to the maximum order of partial derivatives  $DI(f)$  depends upon.

## 4.3 Three Independent Sets of Image Differential Invariants

The letters  $O$  and  $D$  are used to represent the order and the degree of arbitrary differential invariants. When

$O, D \in \{1, 2, 3, 4\}$ , we construct all Euclidean differential invariants by using Eq.(49), and discuss the independence of them. The independent set  $DIS_{(O,D)}^I$  is obtained where  $O, D \in \{3, 4\}$  and  $I \in \{LI, IR, FI\}$ . Note that the order (degree) of any Euclidean differential invariants in  $DIS_{(O,D)}^I$  is less than or equal to  $O(D)$ . We have defined the linearly independence ( $LI$ ), irreducibility ( $IR$ ) and functional independence ( $FI$ ) of image differential invariants in Sect.2.6. And the letter  $I$  denotes the independence of invariants in the set  $DIS_{(O,D)}^I$ .

The construction formulas of 230 Euclidean differential invariants in  $DIS_{(4,4)}^{LI}$  are listed in Table. 4 and Table. 5. In the following, we use  $DI_n$  to represent the invariant generated by using the  $n$ th formulas, where  $n \in \{1, 2, \dots, 230\}$ . Obviously, at most four different points are employed by  $F_{i_p, j_p}$  and  $G_{s_q, t_q}$  in each formula, which ensures the degree of any invariants in  $DIS_{(4,4)}^{LI}$  is less than or equal to 4. Also, we can find any points appears at most four times in each formula. Thus, the order of any invariants in the set is also less than or equal to 4.

There are 134 invariants in  $DI_{(4,4)}^{LI}$  which can be expressed as the polynomial functions of others. These polynomial relations are listed in Table. 6 and Table. 7. This implied  $(230 - 134) = 96$  Euclidean differential invariants in the set  $DI_{(4,4)}^{IR}$ .

In Table. 8, we acquire 12 independent sets of Euclidean differential invariants by setting the different values of  $O, D$  and  $I$ . The number of invariants in each set is listed in Table. 9. When fixing the value of  $O$  and increasing  $D$  from 3 to 4, we find the number of invariants in the functional independent set does not change. Thus,  $DIS_{3,4}^{FI} = DIS_{3,3}^{FI}$  and  $DIS_{4,4}^{FI} = DIS_{4,3}^{FI}$ . In addition, we can get 14 partial derivatives  $\frac{\partial^{i+j} f}{\partial x^i \partial y^j}$  when  $i, j \in \{0, 1, 2, 3, 4\}$  and  $1 \leq (i+j) \leq 4$ . Thus, in theory, there should be 14 differential invariants in  $DIS_{(4,D)}^{FI}$ . However, the number of invariants in the set  $DIS_{(4,3)}^{FI}$  and  $DIS_{(4,4)}^{FI}$  is only 13. This finding was also reported by Florack et al. (1993; 2008).

The explicit representations of all Euclidean differential invariants in  $DIS_{(4,3)}^{IR}$  are presented in Table. 10, where  $f_{ij}$  denotes  $\frac{\partial^{i+j} f}{\partial x^i \partial y^j}$ . Obviously, they are all homogeneous polynomials of partial derivatives. And the better part of them don't depend upon the first partial derivatives, such as  $DI_1, DI_2$  and  $DI_4$ . This indicates that our method can generate more general differential invariants than the methods proposed by Olver and Florack et al.

#### 4.4 Image Differential Invariants for the Action of Complicated Geometric Transformations

It should be noted that we don't find the general method to generate image differential invariants for the action of complicated transformation groups, such as 2D projective transformation group defined by Eq.(4).

But we know that all projective differential invariants are also invariant under 2D Euclidean transform, which means they can be expressed as the functions of Euclidean differential invariants generated by Eq.(49). In fact,  $DI_3, DI_8, DI_{18}, DI_{22}, DI_{37}, DI_{103}, DI_{147}$  and  $DI_{161}$  are relative affine differential invariants. Furthermore, Li and Mo et al. have proved that  $DI_8$  is also a relative projective differential invariant. Zhang et al. recently proposed that  $\frac{DI_1}{DI_2}$  is an absolute differential invariant for 2D mobius transformations.

We have reason to believe that more image differential invariants which are invariant under complicated 2D transforms can be obtained, because our new method can generate image Euclidean, similarity and affine differential invariants quite easily.

#### 4.5 The Construction of 3D Differential Invariants

The fundamental differential operators defined by Eq.(45) can also be extended to generate 3D differential invariants of the function  $f(x, y, z)$ :

$$\begin{aligned} F_{i,j,k} &= \frac{\partial^2}{\partial x_i \partial x_j} + \frac{\partial^2}{\partial y_i \partial y_j} + \frac{\partial^2}{\partial z_i \partial z_j} \\ G_{i,j,k} &= \begin{vmatrix} \frac{\partial}{\partial x_i} & \frac{\partial}{\partial y_i} & \frac{\partial}{\partial z_i} \\ \frac{\partial}{\partial x_j} & \frac{\partial}{\partial y_j} & \frac{\partial}{\partial z_j} \\ \frac{\partial}{\partial x_k} & \frac{\partial}{\partial y_k} & \frac{\partial}{\partial z_k} \end{vmatrix} \\ &= \frac{\partial^3}{\partial x_i \partial y_j \partial z_k} - \frac{\partial^3}{\partial x_i \partial y_k \partial z_j} - \frac{\partial^3}{\partial x_j \partial y_i \partial z_k} \\ &\quad + \frac{\partial^3}{\partial x_j \partial y_k \partial z_i} + \frac{\partial^3}{\partial x_k \partial y_i \partial z_j} - \frac{\partial^3}{\partial x_k \partial y_j \partial z_i} \end{aligned} \quad (55)$$

Suppose the function  $f(x, y, z) : \Omega \subset \mathbb{N}^+ \times \mathbb{N}^+ \times \mathbb{N}^+ \rightarrow \mathbb{R}$  has infinite order partial derivatives. We transform it to  $h(u, v, w) : \Omega' \subset \mathbb{N}^+ \times \mathbb{N}^+ \times \mathbb{N}^+ \rightarrow \mathbb{R}$  using the 3D transformation  $g$ .  $(u_k(x_k, y_k, z_k), v_k(x_k, y_k, z_k), w_k(x_k, y_k, z_k)) \in \Omega'$  is the corresponding point of  $(x_k, y_k, z_k) \in \Omega$ , where  $k \in \{1, 2, \dots, n\}$ . We define the function  $F = f(x_1, y_1, z_1) \cdot f(x_2, y_2, z_2) \cdot \dots \cdot f(x_n, y_n, z_n)$ . The differential invariant of  $F$  is defined by:

$$\begin{aligned} DI(F) &= (F_{i_p, j_p, k_p} \circ \dots \circ F_{i_p, j_p, k_p} \circ \dots \circ F_{i_1, j_1, k_1} \\ &\quad \circ G_{r_q, s_q, t_q} \circ \dots \circ G_{r_q, s_q, t_q} \circ \dots \circ G_{r_1, s_1, t_1}, F) \end{aligned} \quad (56)$$

Table 4: The construction formulas of Euclidean differential invariants in  $DI_{(4,4)}^{LI}$ .

No	GF	No	GF	No	GF	No	GF
1	$F_{1,1}$	2	$F_{1,2}$	3	$G_{1,2} \circ G_{1,2}$	4	$F_{1,1} \circ F_{1,1}$
5	$F_{1,1} \circ F_{2,2}$	6	$F_{1,2} \circ F_{1,3}$	7	$F_{1,2} \circ F_{3,4}$	8	$G_{1,2} \circ G_{1,3}$
9	$F_{1,1} \circ F_{1,2}$	10	$F_{1,1} \circ G_{1,2}$	11	$F_{1,2} \circ G_{1,3}$	12	$F_{1,1} \circ F_{2,2} \circ F_{3,3}$
13	$F_{1,2} \circ F_{1,2} \circ F_{1,2}$	14	$F_{1,2} \circ F_{1,3} \circ F_{1,4}$	15	$F_{1,2} \circ F_{1,3} \circ F_{2,3}$	16	$F_{1,2} \circ G_{1,2} \circ G_{1,2}$
17	$F_{1,2} \circ G_{1,3} \circ G_{3,4}$	18	$G_{1,2} \circ G_{1,3} \circ G_{1,4}$	19	$F_{1,1} \circ F_{2,2} \circ F_{3,3} \circ F_{4,4}$	20	$F_{1,2} \circ F_{1,2} \circ F_{1,2} \circ F_{1,2}$
21	$F_{1,1} \circ F_{2,3} \circ G_{1,2}$ $\circ G_{1,3} \circ G_{2,3}^2$	22	$G_{1,2} \circ G_{1,2} \circ G_{1,3}$ $\circ G_{2,4} \circ G_{3,4} \circ G_{3,4}$	23	$F_{1,1} \circ F_{1,1} \circ F_{2,2}$	24	$F_{1,1} \circ F_{1,1} \circ F_{2,3}$
25	$F_{1,1} \circ F_{1,2} \circ F_{1,2}$	26	$F_{1,1} \circ F_{1,2} \circ F_{1,3}$	27	$F_{1,1} \circ F_{2,2} \circ F_{3,4}$	28	$F_{1,1} \circ F_{2,3} \circ F_{2,4}$
29	$F_{1,2} \circ F_{1,2} \circ F_{1,3}$	30	$F_{1,1} \circ F_{1,2} \circ G_{1,2}$	31	$F_{1,1} \circ F_{1,2} \circ G_{1,3}$	32	$F_{1,1} \circ F_{2,3} \circ G_{2,4}$
33	$F_{1,2} \circ F_{1,2} \circ G_{1,3}$	34	$F_{1,2} \circ F_{1,3} \circ G_{1,4}$	35	$F_{1,2} \circ G_{1,3} \circ G_{1,3}$	36	$F_{1,2} \circ G_{1,3} \circ G_{1,4}$
37	$G_{1,2} \circ G_{1,2} \circ G_{1,3}$	38	$F_{1,1} \circ F_{1,1} \circ F_{2,2}$ $\circ F_{2,2}$	39	$F_{1,2} \circ F_{1,2} \circ F_{1,3} \circ F_{1,3}$	40	$F_{1,2} \circ F_{1,2} \circ F_{3,4} \circ F_{3,4}$
41	$F_{1,2} \circ F_{1,3} \circ F_{2,4}$ $\circ F_{3,4}$	42	$F_{1,2} \circ F_{3,4} \circ G_{1,3}$ $\circ G_{1,3} \circ G_{1,3} \circ G_{2,4}$	43	$F_{1,2} \circ F_{3,4} \circ G_{1,3}$ $\circ G_{1,3} \circ G_{1,3} \circ G_{2,4}$ $\circ G_{2,4} \circ G_{2,4}$	44	$F_{1,1} \circ F_{2,2} \circ G_{1,2}$ $\circ G_{1,2}$
45	$F_{1,1} \circ F_{1,2} \circ F_{2,3}$	46	$F_{1,1} \circ F_{1,2} \circ G_{2,3}$	47	$F_{1,1} \circ F_{2,3} \circ F_{2,3}$ $\circ F_{2,3}$	48	$F_{1,1} \circ F_{2,3} \circ F_{2,3}$ $\circ G_{1,2}$
49	$F_{1,1} \circ F_{1,2} \circ G_{2,3}$ $\circ G_{3,4}$	50	$F_{1,1} \circ F_{1,1} \circ F_{2,2}$ $\circ F_{3,3}$	51	$F_{1,1} \circ F_{1,1} \circ F_{2,3}$ $\circ F_{2,3}$	52	$F_{1,1} \circ F_{1,1} \circ F_{2,3}$ $\circ F_{2,4}$
53	$F_{1,2} \circ F_{1,2} \circ F_{1,3}$ $\circ F_{1,4}$	54	$F_{1,2} \circ F_{1,2} \circ F_{1,3}$ $\circ F_{2,3}$	55	$F_{1,1} \circ F_{1,1} \circ G_{2,3}$ $\circ G_{2,4}$	56	$F_{1,2} \circ F_{1,2} \circ F_{3,4}$ $\circ F_{3,4} \circ G_{1,3} \circ G_{2,4}$
57	$F_{1,1} \circ F_{1,1} \circ G_{2,3}$ $\circ G_{2,3} \circ G_{2,3} \circ G_{2,3}$	58	$F_{1,1} \circ F_{2,2} \circ G_{3,4}$ $\circ G_{3,4} \circ G_{3,4} \circ G_{3,4}$	59	$F_{1,1} \circ F_{1,2} \circ F_{3,3}$ $\circ F_{3,4}$	60	$F_{1,2} \circ F_{1,2} \circ F_{1,3}$ $\circ F_{3,4}$
61	$F_{1,1} \circ F_{1,2} \circ F_{2,3}$ $\circ G_{2,4}$	62	$F_{1,1} \circ F_{2,3} \circ G_{1,2}$ $\circ G_{2,3}$	63	$F_{1,2} \circ F_{1,2} \circ F_{1,2}$ $\circ F_{1,2} \circ F_{3,4}$	64	$F_{1,1} \circ F_{1,1} \circ F_{2,2}$ $\circ F_{2,2} \circ F_{3,3} \circ F_{3,3}$
65	$F_{1,2} \circ F_{1,2} \circ F_{1,2}$ $\circ F_{3,4} \circ F_{3,4} \circ F_{3,4}$	66	$F_{1,2} \circ F_{1,2} \circ F_{1,3}$ $\circ F_{1,3} \circ F_{2,3} \circ F_{2,3}$	67	$F_{1,2} \circ F_{1,2} \circ F_{1,2}$ $\circ F_{1,2} \circ G_{3,4} \circ G_{3,4}$	68	$F_{1,1} \circ F_{2,2} \circ F_{3,4} \circ G_{1,3}$ $\circ G_{1,4} \circ G_{3,4} \circ G_{3,4}$
69	$F_{1,1} \circ F_{1,2} \circ F_{1,2}$ $\circ F_{3,3}$	70	$F_{1,1} \circ F_{1,2} \circ F_{2,3}$ $\circ F_{2,3}$	71	$F_{1,1} \circ F_{1,2} \circ G_{2,3}$ $\circ G_{2,4}$	72	$F_{1,1} \circ F_{1,1} \circ F_{2,2} \circ F_{2,3}$
73	$F_{1,1} \circ F_{1,2} \circ F_{1,3}$ $\circ F_{4,4}$	74	$F_{1,1} \circ F_{1,2} \circ F_{2,2}$ $\circ F_{3,4}$	75	$F_{1,1} \circ F_{1,2} \circ F_{3,3}$ $\circ F_{4,4}$	76	$F_{1,1} \circ F_{2,3} \circ F_{2,3}$ $\circ F_{2,4}$
77	$F_{1,1} \circ F_{1,1} \circ F_{2,2}$ $\circ G_{2,3}$	78	$F_{1,1} \circ F_{1,2} \circ F_{1,2}$ $\circ G_{2,3}$	79	$F_{1,1} \circ F_{1,2} \circ F_{2,3}$ $\circ G_{1,2}$	80	$F_{1,1} \circ F_{1,2} \circ F_{3,3}$ $\circ G_{1,4}$
81	$F_{1,2} \circ F_{1,2} \circ F_{1,3}$ $\circ G_{1,4}$	82	$F_{1,2} \circ F_{1,2} \circ F_{3,4}$ $\circ G_{1,3}$	83	$F_{1,1} \circ F_{2,3} \circ G_{1,2}$ $\circ G_{1,2}$	84	$F_{1,1} \circ F_{1,1} \circ F_{2,2}$ $\circ F_{2,2} \circ F_{3,3}$
85	$F_{1,1} \circ F_{1,1} \circ F_{2,2}$ $\circ F_{2,2} \circ F_{3,4}$	86	$F_{1,1} \circ F_{1,1} \circ F_{2,2}$ $\circ F_{3,3} \circ F_{4,4}$	87	$F_{1,1} \circ F_{1,1} \circ F_{2,3}$ $\circ F_{2,3} \circ F_{2,3}$	88	$F_{1,1} \circ F_{1,1} \circ F_{2,3}$ $\circ F_{2,4} \circ F_{3,4}$
89	$F_{1,2} \circ F_{1,2} \circ F_{1,3}$ $\circ F_{1,3} \circ F_{2,3}$	90	$F_{1,2} \circ F_{1,2} \circ F_{1,3}$ $\circ F_{3,4} \circ F_{3,4}$	91	$F_{1,1} \circ F_{1,1} \circ F_{2,3}$ $\circ G_{2,3} \circ G_{2,3}$	92	$F_{1,1} \circ F_{1,2} \circ F_{2,3}$ $\circ G_{1,2} \circ G_{2,3}$
93	$F_{1,1} \circ F_{1,2} \circ F_{2,3}$ $\circ G_{1,2} \circ G_{2,4}$	94	$F_{1,1} \circ F_{1,2} \circ F_{2,3}$ $\circ G_{2,3} \circ G_{3,4}$	95	$F_{1,1} \circ F_{1,2} \circ F_{3,3}$ $\circ G_{1,2} \circ G_{2,3}$	96	$F_{1,1} \circ F_{2,3} \circ F_{2,3}$ $\circ G_{1,2} \circ G_{3,4}$
97	$F_{1,1} \circ F_{1,2} \circ F_{1,2}$ $\circ F_{2,3} \circ F_{3,3} \circ G_{2,3}$	98	$F_{1,1} \circ F_{1,2} \circ F_{2,3}$ $\circ F_{2,3} \circ F_{4,4} \circ G_{3,4}$	99	$F_{1,1} \circ F_{1,1} \circ F_{2,2}$ $\circ F_{2,2} \circ G_{3,4} \circ G_{3,4}$	100	$F_{1,2} \circ F_{1,3} \circ F_{2,4}$ $\circ F_{3,4} \circ G_{1,4} \circ G_{1,4}$
101	$F_{1,1} \circ F_{1,2} \circ F_{3,4}$ $\circ G_{2,3} \circ G_{2,3} \circ G_{2,3}$	102	$F_{1,1} \circ F_{1,2} \circ G_{2,3}$ $\circ G_{2,3} \circ G_{2,3} \circ G_{3,4}$	103	$G_{1,2} \circ G_{1,2} \circ G_{1,3}$ $\circ G_{1,4} \circ G_{2,3} \circ G_{2,4}$	104	$F_{1,2} \circ F_{1,2} \circ F_{1,2} \circ G_{3,4}$ $\circ G_{3,4} \circ G_{3,4} \circ G_{3,4}$
105	$F_{1,2} \circ F_{1,3} \circ F_{2,4} \circ G_{1,2}$ $\circ G_{3,4} \circ G_{3,4} \circ G_{3,4}$	106	$F_{1,1} \circ F_{1,2} \circ F_{3,3}$ $\circ G_{2,3}$	107	$F_{1,2} \circ F_{1,2} \circ F_{1,3}$ $\circ F_{2,3} \circ F_{3,4}$	108	$F_{1,2} \circ F_{1,3} \circ F_{1,4}$ $\circ F_{2,3} \circ F_{2,4}$
109	$F_{1,1} \circ F_{1,2} \circ F_{2,3}$ $\circ F_{3,4} \circ G_{2,4}$	110	$F_{1,2} \circ F_{1,3} \circ F_{1,4}$ $\circ F_{2,3} \circ G_{1,4}$	111	$F_{1,1} \circ F_{1,2} \circ F_{3,3}$ $\circ F_{3,4} \circ G_{2,4} \circ G_{2,4}$	112	$F_{1,1} \circ F_{1,2} \circ F_{1,3}$ $\circ F_{2,4}$
113	$F_{1,1} \circ F_{2,2} \circ F_{3,4}$ $\circ F_{3,4} \circ F_{3,4} \circ F_{3,4}$	114	$F_{1,1} \circ F_{1,1} \circ F_{2,2}$ $\circ F_{2,2} \circ F_{3,3} \circ F_{3,3}$ $\circ F_{4,4} \circ F_{4,4}$	115	$F_{1,2} \circ F_{1,2} \circ F_{1,2}$ $\circ F_{1,2} \circ F_{3,4} \circ F_{3,4}$ $\circ F_{3,4} \circ F_{3,4}$	116	$F_{1,1} \circ F_{1,2} \circ F_{2,3}$ $\circ F_{2,3} \circ F_{3,4} \circ F_{4,4}$ $\circ G_{1,3} \circ G_{2,4}$
117	$F_{1,2} \circ F_{1,2} \circ F_{1,2}$ $\circ F_{1,2} \circ G_{3,4} \circ G_{3,4}$ $\circ G_{3,4} \circ G_{3,4}$	118	$F_{1,1} \circ F_{1,2} \circ F_{2,3}$ $\circ G_{3,4}$	119	$F_{1,1} \circ F_{2,2} \circ F_{3,4}$ $\circ G_{1,3}$	120	$F_{1,1} \circ F_{2,2} \circ G_{1,3}$ $\circ G_{3,4}$
121	$F_{1,1} \circ F_{1,1} \circ F_{2,2}$ $\circ F_{2,3} \circ F_{2,3}$	122	$F_{1,1} \circ F_{1,1} \circ F_{2,2}$ $\circ F_{2,3} \circ F_{2,4}$	123	$F_{1,1} \circ F_{1,2} \circ F_{1,2}$ $\circ F_{2,2} \circ F_{3,3}$	124	$F_{1,1} \circ F_{1,2} \circ F_{1,2}$ $\circ F_{2,2} \circ F_{3,4}$
125	$F_{1,1} \circ F_{1,2} \circ F_{1,2}$ $\circ F_{3,3} \circ F_{4,4}$	126	$F_{1,1}^2 F_{2,2} F_{2,3} G_{2,3}$	127	$F_{1,1} F_{1,2} F_{2,3} F_{3,4}$ $\cdot G_{1,4}$	128	$F_{1,1} F_{1,2}^2 F_{2,3} F_{3,4}$ $\cdot G_{2,4}$
129	$F_{1,1} \circ F_{1,2} \circ F_{2,3}$ $\circ F_{2,3} \circ F_{4,4} \circ G_{1,2}$	130	$F_{1,1} \circ F_{1,2} \circ F_{2,3}$ $\circ F_{2,3} \circ F_{3,4} \circ F_{4,4}$ $\circ G_{1,2} \circ G_{3,4}$	131	$F_{1,1} \circ F_{1,1} \circ F_{2,2}$ $\circ F_{2,2} \circ G_{3,4} \circ G_{3,4}$ $\circ G_{3,4} \circ G_{3,4}$	132	$F_{1,1} \circ F_{1,1} \circ F_{2,3}$ $\circ F_{2,3} \circ F_{2,4}$

Table 5: The construction formulas of Euclidean differential invariants in  $DI_{(4,4)}^{LI}$ . (Continued)

No	GF	No	GF	No	GF	No	GF
133	$F_{1,1} \circ F_{1,2} \circ F_{1,2} \circ F_{3,4} \circ F_{3,4}$	134	$F_{1,1} \circ F_{1,2} \circ F_{2,2} \circ F_{3,3} \circ F_{4,4}$	135	$F_{1,1} \circ F_{1,2} \circ F_{3,4} \circ F_{3,4} \circ G_{1,2}$	136	$F_{1,1} \circ F_{1,1} \circ F_{2,2} \circ F_{2,2} \circ F_{3,3} \circ F_{4,4}$
137	$F_{1,1} \circ F_{1,1} \circ F_{2,3} \circ F_{2,3} \circ F_{2,4} \circ F_{2,4}$	138	$F_{1,1} \circ F_{1,1} \circ F_{2,3} \circ F_{2,4} \circ G_{3,4} \circ G_{3,4}$	139	$F_{1,2} \circ F_{1,2} \circ F_{1,3} \circ F_{1,4} \circ G_{2,3} \circ G_{3,4}$	140	$F_{1,2} \circ F_{1,2} \circ F_{1,3} \circ F_{3,4} \circ G_{1,4} \circ G_{2,3}$
141	$F_{1,2} \circ F_{1,2} \circ F_{1,3} \circ F_{3,4} \circ G_{2,3} \circ G_{2,3}$	142	$F_{1,2} \circ F_{1,2} \circ F_{1,3} \circ G_{2,3} \circ G_{2,3} \circ G_{3,4}$	143	$F_{1,1} \circ F_{1,1} \circ G_{2,3} \circ G_{2,3} \circ G_{2,4} \circ G_{2,4}$	144	$F_{1,1} \circ F_{1,1} \circ G_{2,3} \circ G_{2,3} \circ G_{2,4} \circ G_{3,4}$
145	$F_{1,2} \circ F_{1,2} \circ G_{1,3} \circ G_{1,4} \circ G_{3,4} \circ G_{3,4}$	146	$F_{1,2} \circ G_{1,3} \circ G_{1,3} \circ G_{1,4} \circ G_{3,4} \circ G_{3,4}$	147	$G_{1,2} \circ G_{1,2} \circ G_{1,3} \circ G_{1,3} \circ G_{2,3} \circ G_{2,4}$	148	$F_{1,1} \circ F_{1,2} \circ F_{1,3} \circ F_{2,4} \circ G_{3,4} \circ G_{3,4} \circ G_{3,4}$
149	$F_{1,1} \circ F_{1,1} \circ F_{2,2} \circ G_{3,4} \circ G_{3,4} \circ G_{3,4} \circ G_{3,4}$	150	$F_{1,1} \circ F_{1,2} \circ F_{1,2} \circ G_{3,4} \circ G_{3,4} \circ G_{3,4} \circ G_{3,4}$	151	$F_{1,1} \circ F_{1,2} \circ F_{1,2} \circ F_{2,3} \circ F_{3,3}$	152	$F_{1,1} \circ F_{1,2} \circ F_{2,3} \circ F_{2,3} \circ F_{4,4}$
153	$F_{1,2} \circ F_{1,2} \circ F_{1,3} \circ F_{2,4} \circ G_{1,4}$	154	$F_{1,1} \circ F_{2,3} \circ F_{2,3} \circ G_{1,4} \circ G_{2,4}$	155	$F_{1,1} \circ F_{2,3} \circ F_{2,4} \circ G_{1,3} \circ G_{2,4}$	156	$F_{1,1} \circ F_{1,2} \circ F_{3,4} \circ F_{3,4} \circ F_{3,4} \circ F_{3,4}$
157	$F_{1,2} \circ F_{1,2} \circ F_{1,3} \circ F_{1,3} \circ F_{2,4} \circ F_{3,4}$	158	$F_{1,1} \circ F_{2,3} \circ F_{2,3} \circ F_{2,3} \circ F_{2,3} \circ G_{1,4}$	159	$F_{1,2} \circ F_{1,2} \circ F_{1,3} \circ F_{1,3} \circ G_{2,4} \circ G_{3,4}$	160	$F_{1,2} \circ F_{1,3} \circ G_{2,4} \circ G_{2,4} \circ G_{3,4} \circ G_{3,4}$
161	$G_{1,2} \circ G_{1,2} \circ G_{1,3} \circ G_{1,3} \circ G_{2,4} \circ G_{3,4}$	162	$F_{1,1} \circ F_{1,1} \circ F_{2,2} \circ F_{2,2} \circ F_{3,3} \circ F_{3,3} \circ F_{4,4}$	163	$F_{1,1} \circ F_{2,3} \circ F_{2,3} \circ F_{2,3} \circ F_{2,4} \circ F_{3,4} \circ F_{3,4}$	164	$F_{1,2} \circ F_{1,2} \circ F_{1,2} \circ F_{1,2} \circ F_{3,4} \circ F_{3,4} \circ F_{3,4}$
165	$F_{1,2} \circ F_{1,2} \circ F_{1,2} \circ F_{1,3} \circ F_{3,4} \circ F_{3,4} \circ F_{3,4}$	166	$F_{1,2} \circ F_{1,2} \circ F_{1,2} \circ F_{1,2} \circ F_{3,4} \circ G_{3,4} \circ G_{3,4}$	167	$F_{1,1} \circ F_{1,2} \circ F_{2,3} \circ F_{3,4} \circ F_{3,4} \circ G_{1,3}$	168	$F_{1,1} \circ F_{1,1} \circ F_{2,2} \circ F_{2,3} \circ F_{3,4}$
169	$F_{1,1} \circ F_{1,1} \circ F_{2,2} \circ F_{2,3} \circ F_{4,4}$	170	$F_{1,1} \circ F_{1,2} \circ F_{1,2} \circ F_{2,3} \circ F_{3,4}$	171	$F_{1,1} \circ F_{1,2} \circ F_{1,2} \circ F_{2,3} \circ F_{4,4}$	172	$F_{1,1} \circ F_{1,2} \circ F_{1,2} \circ F_{3,3} \circ F_{3,4}$
173	$F_{1,1} \circ F_{1,2} \circ F_{1,3} \circ F_{2,4} \circ F_{2,4}$	174	$F_{1,1} \circ F_{1,2} \circ F_{2,3} \circ F_{2,3} \circ F_{2,4}$	175	$F_{1,1} \circ F_{1,1} \circ F_{2,2} \circ F_{2,3} \circ G_{3,4}$	176	$F_{1,1} \circ F_{1,1} \circ F_{2,2} \circ F_{3,3} \circ G_{2,4}$
177	$F_{1,2} \circ F_{1,2} \circ F_{1,3} \circ F_{3,4} \circ G_{1,2}$	178	$F_{1,2} \circ F_{1,2} \circ F_{1,3} \circ F_{3,4} \circ G_{1,3}$	179	$F_{1,1} \circ F_{1,2} \circ F_{1,3} \circ G_{2,4} \circ G_{2,4}$	180	$F_{1,1} \circ F_{1,1} \circ F_{2,2} \circ F_{2,2} \circ F_{3,3} \circ F_{3,4}$
181	$F_{1,1} \circ F_{1,1} \circ F_{2,2} \circ F_{3,4} \circ F_{3,4} \circ F_{3,4}$	182	$F_{1,1} \circ F_{1,1} \circ F_{2,3} \circ F_{2,3} \circ F_{2,3} \circ F_{2,4}$	183	$F_{1,1} \circ F_{1,2} \circ F_{1,2} \circ F_{3,4} \circ F_{3,4} \circ F_{3,4}$	184	$F_{1,2} \circ F_{1,2} \circ F_{1,2} \circ F_{1,3} \circ F_{2,3} \circ F_{3,4}$
185	$F_{1,1} \circ F_{1,1} \circ F_{2,2} \circ F_{2,2} \circ F_{3,3} \circ G_{3,4}$	186	$F_{1,1} \circ F_{1,1} \circ F_{2,2} \circ F_{3,4} \circ F_{3,4} \circ G_{2,3}$	187	$F_{1,1} \circ F_{1,1} \circ F_{2,3} \circ F_{2,3} \circ F_{2,3} \circ G_{2,4}$	188	$F_{1,1} \circ F_{1,2} \circ F_{1,2} \circ F_{2,3} \circ G_{2,3}$
189	$F_{1,1} \circ F_{1,2} \circ F_{1,2} \circ F_{3,3} \circ F_{4,4} \circ G_{2,3}$	190	$F_{1,1} \circ F_{1,2} \circ F_{1,2} \circ F_{3,4} \circ F_{3,4} \circ G_{2,3}$	191	$F_{1,1} \circ F_{1,2} \circ F_{2,3} \circ F_{2,3} \circ F_{3,4} \circ G_{1,2}$	192	$F_{1,1} \circ F_{1,2} \circ F_{3,4} \circ F_{3,4} \circ G_{1,2}$
193	$F_{1,1} \circ F_{2,3} \circ F_{2,3} \circ F_{2,4} \circ F_{2,4} \circ G_{1,3}$	194	$F_{1,2} \circ F_{1,2} \circ F_{1,2} \circ F_{1,3} \circ F_{2,3} \circ G_{3,4}$	195	$F_{1,2} \circ F_{1,2} \circ F_{1,2} \circ F_{3,4} \circ F_{3,4} \circ G_{1,3}$	196	$F_{1,1} \circ F_{1,2} \circ F_{1,2} \circ F_{2,3} \circ G_{2,3} \circ G_{3,4}$
197	$F_{1,1} \circ F_{1,2} \circ F_{2,3} \circ F_{2,3} \circ G_{1,2} \circ G_{3,4}$	198	$F_{1,2} \circ F_{1,2} \circ F_{1,2} \circ G_{1,3} \circ G_{3,4} \circ G_{3,4}$	199	$F_{1,2} \circ F_{1,2} \circ F_{1,3} \circ G_{3,4} \circ G_{3,4} \circ G_{3,4}$	200	$F_{1,2} \circ G_{1,3} \circ G_{1,3} \circ G_{1,3} \circ G_{2,4} \circ G_{2,4}$
201	$F_{1,1} \circ F_{1,1} \circ F_{2,2} \circ F_{2,2} \circ F_{3,4} \circ F_{3,4} \circ F_{3,4}$	202	$F_{1,1} \circ F_{1,2} \circ F_{1,2} \circ F_{2,3} \circ F_{2,3} \circ F_{4,4} \circ G_{3,4}$	203	$F_{1,1} \circ F_{1,2} \circ F_{1,2} \circ F_{2,3} \circ F_{3,3} \circ F_{4,4} \circ G_{2,3}$	204	$F_{1,1} \circ F_{1,2} \circ F_{1,3} \circ F_{2,3} \circ F_{2,4} \circ F_{2,4} \circ G_{3,4}$
205	$F_{1,1} \circ F_{1,1} \circ F_{2,2} \circ F_{2,2} \circ F_{3,4} \circ G_{3,4} \circ G_{3,4}$	206	$F_{1,1} \circ F_{1,2} \circ F_{1,2} \circ F_{2,3} \circ F_{4,4} \circ G_{2,3} \circ G_{3,4}$	207	$F_{1,1} \circ F_{1,2} \circ F_{2,3} \circ F_{2,3} \circ F_{4,4} \circ G_{1,2} \circ G_{3,4}$	208	$F_{1,2} \circ F_{1,2} \circ F_{1,3} \circ F_{2,4} \circ F_{3,4} \circ G_{1,4} \circ G_{3,4}$
209	$F_{1,2} \circ F_{1,2} \circ F_{1,2} \circ G_{1,3} \circ G_{3,4} \circ G_{3,4} \circ G_{3,4}$	210	$F_{1,1} \circ F_{1,2} \circ F_{1,3} \circ F_{2,3} \circ F_{2,4} \circ G_{2,4}$	211	$F_{1,1} \circ F_{1,2} \circ F_{1,2} \circ F_{2,3} \circ F_{3,4} \circ F_{3,4} \circ G_{2,3}$	212	$F_{1,1} \circ F_{1,2} \circ F_{2,3} \circ F_{2,3} \circ F_{3,4} \circ F_{3,4} \circ G_{1,2}$
213	$F_{1,2} \circ F_{1,2} \circ F_{1,2} \circ F_{1,3} \circ G_{3,4} \circ G_{3,4} \circ G_{3,4}$	214	$F_{1,1} \circ F_{1,1} \circ F_{2,2} \circ F_{2,3} \circ F_{2,3} \circ F_{3,4} \circ F_{4,4} \circ G_{3,4}$	215	$F_{1,1} \circ F_{1,1} \circ F_{2,3} \circ F_{2,3} \circ F_{2,4} \circ F_{3,4}$	216	$F_{1,2} \circ F_{1,2} \circ F_{1,3} \circ F_{1,4} \circ F_{3,4} \circ F_{3,4}$
217	$F_{1,2} \circ F_{1,2} \circ F_{1,2} \circ F_{1,3} \circ F_{3,4} \circ G_{3,4}$	218	$F_{1,1} \circ F_{1,2} \circ F_{1,2} \circ F_{2,3} \circ F_{3,4} \circ F_{3,4} \circ G_{2,4}$	219	$F_{1,1} \circ F_{1,2} \circ F_{2,3} \circ F_{2,3} \circ F_{3,4} \circ F_{4,4} \circ G_{1,2}$	220	$F_{1,1} \circ F_{1,2} \circ F_{1,3} \circ F_{2,4} \circ F_{3,4} \circ G_{2,3} \circ G_{2,3}$
221	$F_{1,2} \circ F_{1,2} \circ F_{1,3} \circ F_{1,4} \circ F_{2,3} \circ G_{2,3} \circ G_{3,4}$	222	$F_{1,2} \circ F_{1,2} \circ F_{1,3} \circ F_{2,4} \circ F_{3,4} \circ G_{1,4} \circ G_{2,3}$	223	$F_{1,2} \circ F_{1,2} \circ F_{1,3} \circ F_{3,4} \circ F_{3,4} \circ G_{1,4} \circ G_{2,3}$	224	$F_{1,1} \circ F_{1,1} \circ F_{2,2} \circ F_{2,3} \circ F_{3,4} \circ G_{3,4}$
225	$F_{1,1} \circ F_{1,1} \circ F_{2,2} \circ F_{2,2} \circ F_{3,3} \circ F_{3,4} \circ F_{3,4}$	226	$F_{1,1} \circ F_{1,2} \circ F_{2,2} \circ F_{3,4} \circ F_{3,4} \circ F_{3,4} \circ G_{1,3}$	227	$F_{1,1} \circ F_{1,2} \circ F_{3,4} \circ F_{3,4} \circ F_{3,4} \circ F_{3,4} \circ G_{1,2}$	228	$F_{1,1} \circ F_{1,2} \circ F_{3,3} \circ F_{3,4} \circ G_{1,4}$
229	$F_{1,1} \circ F_{1,2} \circ F_{3,3} \circ F_{4,4} \circ G_{1,3}$	230	$F_{1,1} \circ F_{1,2} \circ F_{1,2} \circ F_{2,3} \circ F_{3,4} \circ F_{3,4} \circ G_{3,4}$	/	/	/	/

Table 6: The polynomial relations of Euclidean differential invariants in  $DI_{s(4,4)}^{LI}$ .

Polynomial Relation	Polynomial Relation
$DI_5 = DI_1^2$	$DI_7 = DI_2^2$
$DI_8 = DI_1 DI_2 - DI_6$	$DI_{12} = DI_1^3$
$DI_{15} = DI_1^3 - \frac{3}{2} DI_1 DI_3$	$DI_{17} = -\frac{1}{2} DI_2 DI_3$
$DI_{19} = DI_1^4$	$DI_{23} = DI_1 DI_4$
$DI_{24} = DI_2 DI_4$	$DI_{27} = DI_1^2 DI_2$
$DI_{28} = DI_1 DI_6$	$DI_{32} = DI_1 DI_{11}$
$DI_{34} = DI_2 DI_{10} - DI_{18}$	$DI_{35} = DI_1 DI_9 - DI_{29}$
$DI_{36} = DI_2 DI_9 - DI_{14}$	$DI_{37} = DI_1 DI_{10} - DI_{33}$
$DI_{38} = DI_4^2$	$DI_{40} = DI_3^2 + DI_1^2 (DI_1^2 - 2DI_3)$
$DI_{41} = DI_1^2 (DI_1^2 - 2DI_3) + \frac{1}{2} DI_3$	$DI_{42} = \frac{1}{2} DI_3 (2DI_{44} + DI_{20} - DI_4^2)$
$DI_{43} = 2DI_{44} (DI_{44} - DI_4^2) + DI_{20} (2DI_{44} + \frac{1}{2} DI_{20} - DI_4^2) + \frac{1}{2} DI_4^4$	$DI_{47} = DI_1 DI_{13}$
$DI_{49} = -\frac{1}{2} DI_3 DI_9$	$DI_{50} = DI_1^2 DI_4$
$DI_{51} = DI_4 DI_5 - DI_3 DI_4$	$DI_{52} = DI_4 DI_6$
$DI_{55} = DI_4 (DI_1 DI_2 - DI_6)$	$DI_{56} = DI_{16}^2 - DI_{22}$
$DI_{57} = DI_4 (DI_{20} + 2DI_{44} - DI_4^2)$	$DI_{58} = DI_1^2 (2DI_{44} + DI_{20} - DI_4^2)$
$DI_{59} = DI_9^2$	$DI_{63} = DI_2 DI_{20}$
$DI_{64} = DI_4^3$	$DI_{65} = DI_{13}^2$
$DI_{66} = \frac{1}{2} DI_4 (3DI_{20} - DI_4^2) + \frac{3}{2} DI_{21}$	$DI_{67} = DI_3 DI_{20}$
$DI_{68} = DI_1 DI_{21}$	$DI_{69} = DI_1 DI_{25}$
$DI_{70} = \frac{1}{2} DI_1 DI_{16} + DI_{54}$	$DI_{72} = DI_4 DI_9$
$DI_{73} = DI_1 DI_{26}$	$DI_{74} = DI_9^2 + DI_{10}^2$
$DI_{75} = DI_1^2 DI_9$	$DI_{76} = DI_1 DI_{29}$
$DI_{77} = DI_4 DI_{10}$	$DI_{84} = DI_4^2 DI_1$
$DI_{85} = DI_4^2 DI_2$	$DI_{86} = DI_1^3 DI_4$
$DI_{87} = DI_4 DI_{13}$	$DI_{88} = DI_1 DI_4 (DI_1^2 - \frac{3}{2} DI_3)$
$DI_{91} = DI_4 DI_{16}$	$DI_{94} = -\frac{1}{2} DI_9 DI_{16}$
$DI_{99} = DI_4^2 DI_3$	$DI_{100} = \frac{1}{4} DI_1^2 (DI_4^2 - DI_{44} - DI_{20}) + \frac{1}{4} DI_4 (2DI_1 DI_{25} - DI_4 DI_3 - 2DI_{39}) - DI_1 DI_{92} - \frac{1}{2} DI_{30}^2$
$DI_{101} = \frac{1}{2} DI_{10} (2DI_{44} + DI_{20} - DI_4^2)$	$DI_{102} = \frac{1}{2} DI_9 (DI_4^2 - DI_{20} - 2DI_{44})$
$DI_{103} = \frac{1}{4} DI_1^2 (DI_4^2 - DI_{44} - DI_{20}) + \frac{1}{4} DI_4 (2DI_1 DI_{25} - DI_4 DI_3 - 2DI_{39}) + DI_1 DI_{92} - \frac{1}{2} DI_{30}^2$	$DI_{104} = DI_{13} (2DI_{44} + DI_{20} - DI_4^2)$
$DI_{105} = \frac{1}{2} DI_{16} (2DI_{44} - DI_4^2 + DI_{20})$	$DI_{107} = DI_{96} - \frac{1}{2} DI_9 (DI_{16} - 2DI_{13})$
$DI_{108} = DI_{90} - \frac{1}{2} DI_3 DI_{16}$	$DI_{109} = -DI_1 (DI_{48} + DI_{106})$
$DI_{111} = \frac{1}{2} DI_{16} (2DI_{13} + 3DI_{16}) - DI_{22}$	$DI_{112} = \frac{1}{2} DI_2 DI_{25} + \frac{1}{2} DI_1 DI_{26} - \frac{1}{2} DI_4 (DI_1 DI_2 - DI_6)$
$DI_{113} = DI_1^2 DI_{20}$	$DI_{114} = DI_4^4$
$DI_{115} = DI_{20}^2$	$DI_{116} = \frac{1}{2} DI_4 DI_{21}$
$DI_{117} = DI_{20} (2DI_{44} + DI_{20} - DI_4^2)$	$DI_{120} = DI_1 (DI_{45} - DI_1 DI_9)$
$DI_{121} = DI_4 DI_{25}$	$DI_{122} = DI_4 DI_{26}$
$DI_{123} = DI_1 (DI_4^2 - DI_{44})$	$DI_{124} = DI_2 (DI_4^2 - DI_{44})$
$DI_{125} = DI_1^2 DI_{25}$	$DI_{126} = DI_4 DI_{30}$
$DI_{127} = DI_{30} (DI_1^2 - \frac{1}{2} DI_3)$	$DI_{129} = DI_1 DI_4 DI_{30} - DI_{128}$
$DI_{130} = \frac{1}{2} DI_{44} (DI_{44} - DI_4^2 + DI_{20}) + \frac{1}{2} DI_4 DI_{21}$	$DI_{131} = DI_4^2 (2DI_{44} + DI_{20} - DI_4^2)$
$DI_{132} = DI_4 DI_{29}$	$DI_{133} = DI_{25} (DI_1^2 - DI_3)$
$DI_{134} = DI_1^2 (DI_{13} + DI_{16})$	$DI_{135} = DI_{30} (DI_1^2 - DI_3)$
$DI_{136} = DI_1^2 DI_4^2$	$DI_{137} = DI_4 DI_{39}$
$DI_{138} = DI_4 (\frac{1}{2} DI_1 DI_{16} - DI_{62})$	$DI_{140} = DI_{139} + \frac{1}{2} DI_1 (DI_4 DI_{16} - 2DI_{95})$
$DI_{143} = DI_1^2 (DI_4^2 - DI_{44}) + DI_3 (2DI_{44} - DI_4^2) + DI_4 DI_{39} - 2DI_{25}^2 - 2DI_{30}^2$	$DI_{144} = DI_4 (DI_{62} + \frac{1}{2} DI_1 DI_{16})$
$DI_{145} = DI_{16} DI_{25} + 2DI_{139}$	$DI_{149} = DI_1 DI_4 (2DI_{44} + DI_{20} - DI_4^2)$
$DI_{150} = DI_{25} (2DI_{44} + DI_{20} - DI_4^2)$	$DI_{152} = DI_1 (DI_{54} + \frac{1}{2} DI_1 DI_{16})$

Table 7: The polynomial relations of Euclidean differential invariants in  $DI_{s(4,4)}^{LI}$ . (Continued)

Polynomial Relation	Polynomial Relation
$DI_{155} = DI_{154} - \frac{1}{2}DI_3(DI_{13} + DI_{16})$	$DI_{156} = DI_9DI_{20}$
$DI_{158} = DI_{10}DI_{20}$	$DI_{159} = DI_1DI_{89} - DI_{157}$
$DI_{161} = -DI_{160} + DI_1(DI_4DI_{16} + DI_{89} + DI_4DI_{13} - 2DI_{151})$	$DI_{162} = DI_1DI_4^3$
$DI_{163} = \frac{1}{2}DI_1(3DI_4DI_{20} + 3DI_{21} - DI_4^3)$	$DI_{164} = DI_{13}DI_{20}$
$DI_{166} = DI_{16}DI_{20}$	$DI_{168} = DI_4DI_{45}$
$DI_{169} = DI_1DI_4DI_9$	$DI_{171} = DI_1(DI_4DI_9 - DI_{83})$
$DI_{172} = DI_9DI_{25}$	$DI_{175} = DI_4DI_{46}$
$DI_{176} = DI_1DI_4DI_{10}$	$DI_{179} = DI_{10}DI_{30} + DI_4(DI_{45} - DI_{29})$ $+ DI_1(DI_4DI_9 - DI_{83}) - 2DI_{170}$ $+ DI_{173}$
$DI_{180} = DI_4^2DI_9$	$DI_{181} = DI_1DI_4DI_{13}$
$DI_{183} = DI_{13}DI_{25}$	$DI_{185} = DI_4^2DI_{10}$
$DI_{186} = DI_4DI_{48}$	$DI_{190} = \frac{1}{2}(DI_{16}DI_{30} + DI_4DI_{48} + DI_{189})$
$DI_{191} = DI_4DI_{79} - DI_{188}$	$DI_{192} = DI_{13}DI_{30}$
$DI_{194} = \frac{1}{2}(-DI_{142} - DI_{146} - DI_{188} + DI_4(2DI_{78}$ $+ DI_{79}) + DI_{10}(DI_{20} - DI_4^2))$	$DI_{197} = -DI_{141} + DI_{147} - 2DI_{184} + DI_9DI_{20}$ $+ DI_4(DI_4DI_9 - 2DI_{83})$
$DI_{201} = DI_4^2DI_{13}$	$DI_{203} = DI_1DI_{97}$
$DI_{205} = DI_4^2DI_{16}$	$DI_{207} = DI_4DI_{95} - DI_{206}$
$DI_{210} = DI_{25}DI_{30} - DI_{167}$	$DI_{212} = 2DI_{148} + DI_{211} - DI_1DI_{97} - DI_{30}DI_{44}$
$DI_{214} = DI_4DI_{97}$	$DI_{215} = DI_4DI_{54}$
$DI_{221} = \frac{1}{4}DI_1DI_{21} + \frac{1}{2}DI_{25}(DI_{44} + DI_{20} - DI_4^2)$	$DI_{222} = -\frac{2}{3}DI_{209} + DI_4(DI_{151} - DI_{89})$ $- \frac{1}{6}DI_{13}(DI_{44} - DI_{20} + DI_4^2)$ $+ \frac{1}{2}DI_{16}(DI_{44} - 2DI_4^2 + DI_{20})$
$DI_{223} = -\frac{1}{6}DI_{13}(2DI_{44} + DI_{20} - DI_4^2)$ $+ DI_{16}(DI_{44} - DI_4^2 + DI_{20}) - DI_4DI_{89}$ $+ DI_{165} + 2DI_{208} - \frac{4}{3}DI_{209}$	$DI_{224} = -DI_4(DI_{48} + DI_{106})$
$DI_{225} = DI_4^2DI_{25}$	$DI_{227} = DI_{20}DI_{30}$

Each point  $(x_k, y_k, z_k)$  is used at least one time by  $F_{i_p, j_p, z_p}$  and  $G(r_q, s_q, t_q)$ .

In fact, we can find the relation  $DI(F) = C \cdot DI'(H)$ , when  $g$  belongs to 3D Euclidean, similarity and affine transformation group. The constant  $C$  is determined by the parameters of  $g$ .  $DI'(H)$  is constructed by:

$$DI'(H) = (F'_{i_p, j_p, k_p} \circ \dots \circ F'_{i_p, j_p, k_p} \circ \dots \circ F'_{i_1, j_1, k_1} \circ G'_{r_q, s_q, t_q} \circ \dots \circ G'_{r_q, s_q, t_q} \circ \dots \circ G'_{r_1, s_1, t_1}, H) \quad (57)$$

where  $H = f(u_1, v_1, w_1) \cdot f(u_2, v_2, w_2) \cdot \dots \cdot f(u_n, v_n, w_n)$  and:

$$F'_{i,j,k} = \frac{\partial^2}{\partial u_i \partial u_j} + \frac{\partial^2}{\partial v_i \partial v_j} + \frac{\partial^2}{\partial w_i \partial w_j}$$

$$G'_{i,j,k} = \frac{\partial^3}{\partial u_i \partial v_j \partial w_k} - \frac{\partial^3}{\partial u_i \partial v_k \partial w_j} - \frac{\partial^3}{\partial u_j \partial v_i \partial w_k} + \frac{\partial^3}{\partial u_j \partial v_k \partial w_i} + \frac{\partial^3}{\partial u_k \partial v_i \partial w_j} - \frac{\partial^3}{\partial u_k \partial v_j \partial w_i}$$

Similar to the proof of the Theorem 2, this relation can also be proved by using the chain's rule for the compound function and the linearity of differential operators  $F_{i,j,k}$  and  $G_{i,j,k}$ . Based on  $DI(F)$ ,  $DI(f)$ , the differential invariant of  $f(x, y)$ , can be obtained by setting  $x_1 = x_2 = \dots = x_n = x$ ,  $y_1 = y_2 = \dots = y_n = y$  and  $z_1 = z_2 = \dots = z_n = z$ .

## 5 Experiment and Discussions

In this section, we conduct some experiments to evaluate the performance of image Euclidean differential invariants generated in Sect.4.3. First, when we use the derivatives of 2D Gaussian function to estimate image partial derivatives, the relation between Euclidean differential invariants and Gaussian-Hermite moment invariants is proposed. Then, the classification experiments are carried out on eight synthetic databases.

Table 8: Twelve independent sets of Euclidean differential invariants when setting different values of  $O, D, I$ .

(O,D)	I=LI	I=IR	I=FI
(3,3)	$DI_1 \sim DI_3, DI_5, DI_6, DI_8 \sim DI_{13}$ , $DI_{15}, DI_{16}, DI_{29}, DI_{33}, DI_{35}, DI_{37}$ , $DI_{45} \sim DI_{48}, DI_{54}, DI_{62}, DI_{70}, DI_{106}$	$DI_1 \sim DI_3, DI_6, DI_9 \sim DI_{11}$ , $DI_{13}, DI_{16}, DI_{29}, DI_{33}, DI_{45}, DI_{46}$ , $DI_{48}, DI_{54}, DI_{62}, DI_{106}$	$DI_1 \sim DI_3, DI_6, DI_9$ , $DI_{10}, DI_{13}, DI_{29}$
(3,4)	$DI_1 \sim DI_3, DI_5 \sim DI_{19}, DI_{22}, DI_{27}$ $\sim DI_{29}, DI_{32} \sim DI_{37}, DI_{40}, DI_{41}, DI_{45}$ $\sim DI_{49}, DI_{54}, DI_{56}, DI_{59} \sim DI_{62}, DI_{65}$ , $DI_{70}, DI_{71}, DI_{74} \sim DI_{76}, DI_{82}, DI_{90}$ , $DI_{94}, DI_{96}, DI_{98}, DI_{106} \sim DI_{109}, DI_{111}$ , $DI_{118} \sim DI_{120}, DI_{134}, DI_{152}, DI_{154}$ , $DI_{155}$	$DI_1 \sim DI_3, DI_6, DI_9 \sim DI_{11}$ , $DI_{13}, DI_{14}, DI_{16}, DI_{18}, DI_{22}$ , $DI_{29}, DI_{33}, DI_{45}, DI_{46}, DI_{48}$ , $DI_{54}, DI_{60} \sim DI_{62}, DI_{71}, DI_{82}$ , $DI_{90}, DI_{96}, DI_{98}, DI_{106}, DI_{118}$ , $DI_{119}, DI_{154}$	$DI_1 \sim DI_3, DI_6, DI_9$ , $DI_{10}, DI_{13}, DI_{29}$
(4,3)	$DI_1 \sim DI_6, DI_8 \sim DI_{13}, DI_{15}, DI_{16}$ , $DI_{20}, DI_{21}, DI_{23} \sim DI_{26}, DI_{29} \sim DI_{31}$ , $DI_{33}, DI_{37} \sim DI_{39}, DI_{44} \sim DI_{48}$ $DI_{50}, DI_{51}, DI_{54}, DI_{57}, DI_{62}, DI_{64}, DI_{66}$ $DI_{69}, DI_{70}, DI_{72}, DI_{77} \sim DI_{79}, DI_{83}$ , $DI_{84}, DI_{87}, DI_{89}, DI_{91}, DI_{92}, DI_{95}, DI_{97}$ , $DI_{106}, DI_{121}, DI_{123}, DI_{126}, DI_{151}$	$DI_1 \sim DI_4, DI_6, DI_9 \sim DI_{11}$ , $DI_{13}, DI_{16}, DI_{20}, DI_{21}, DI_{25}$ , $DI_{26}, DI_{29} \sim DI_{31}, DI_{33}, DI_{39}$ , $DI_{44} \sim DI_{46}, DI_{48}, DI_{54}, DI_{62}$ , $DI_{78}, DI_{79}, DI_{83}, DI_{89}, DI_{92}$ , $DI_{95}, DI_{97}, DI_{106}, DI_{151}$	$DI_1 \sim DI_4, DI_6, DI_9$ , $DI_{10}, DI_{13}, DI_{20}, DI_{21}$ , $DI_{25}, DI_{29}, DI_{30}$
(4,4)	$DI_1 \sim DI_{230}$	$DI_1 \sim DI_4, DI_6, DI_9 \sim DI_{11}$ , $DI_{13}, DI_{14}, DI_{16}, DI_{18}, DI_{20}$ $\sim DI_{22}, DI_{25}, DI_{26}, DI_{29} \sim DI_{31}$ , $DI_{33}, DI_{39}, DI_{44} \sim DI_{46}, DI_{48}$ , $DI_{53}, DI_{54}, DI_{60} \sim DI_{62}, DI_{71}$ , $DI_{78}, DI_{80} \sim DI_{83}, DI_{89}, DI_{90}$ , $DI_{92}, DI_{93}, DI_{95} \sim DI_{98}, DI_{106}$ , $DI_{110}, DI_{118}, DI_{119}, DI_{128}, DI_{139}$ , $DI_{141}, DI_{142}, DI_{146} \sim DI_{148}$ , $DI_{151}, DI_{153}, DI_{154}, DI_{157}, DI_{160}$ , $DI_{165}, DI_{167}, DI_{170}, DI_{173}, DI_{174}$ , $DI_{177}, DI_{178}, DI_{182}, DI_{184}, DI_{187}$ $\sim DI_{189}, DI_{193}, DI_{195}, DI_{196}, DI_{198}$ $\sim DI_{200}, DI_{202}, DI_{204}, DI_{206}, DI_{208}$ , $DI_{209}, DI_{211}, DI_{213}, DI_{216} \sim$ $DI_{220}, DI_{226}, DI_{228} \sim DI_{230}$	$DI_1 \sim DI_4, DI_6, DI_9$ , $DI_{10}, DI_{13}, DI_{20}, DI_{21}$ , $DI_{25}, DI_{29}, DI_{30}$

Table 9: The number of differential invariants in  $DIS_{(O,D)}^I$  where  $O, D \in \{3, 4\}$  and  $I \in \{LI, IR, FI\}$ .

Set	Number	Set	Number
$DIS_{(4,4)}^{LI}$	230	$DIS_{(4,4)}^{IR}$	96
$DIS_{(4,4)}^{FI}$	13	$DIS_{(4,3)}^{LI}$	59
$DIS_{(4,3)}^{IR}$	34	$DIS_{(4,3)}^{FI}$	13
$DIS_{(3,4)}^{LI}$	64	$DIS_{(3,4)}^{IR}$	30
$DIS_{(3,4)}^{FI}$	8	$DIS_{(3,3)}^{LI}$	25
$DIS_{(3,3)}^{IR}$	17	$DIS_{(3,3)}^{FI}$	8

Based on the results, we analyse the effect of various factors on the performance of them in detail. Finally, image patch verification and texture classification experiments are performed on popular real databases. We find that image differential invariants have better per-

formance than some famous handcrafted features in most cases.

### 5.1 The Relation between Image Differential Invariants and Gaussian-Hermite Moment Invariants

As mentioned in Sect.2.2, we have to use Eq.(6) to estimate the numerical value of  $\frac{\partial^{i+j} f}{\partial x^i \partial y^j}$  at the point  $(x_0, y_0)$  because the image  $f(x, y) : \Omega \subset \mathbb{N}^+ \times \mathbb{N}^+ \rightarrow \mathbb{R}$  is a discrete function. We find the relation between the derivatives of  $G(x, y; \sigma) = \frac{1}{2\pi\sigma^2} e^{-\frac{(x-x_0)^2 + (y-y_0)^2}{2\sigma^2}}$  and Gaussian-Hermite polynomials  $\hat{H}_i(x-x_0; \sigma) \hat{H}_j(y-y_0; \sigma)$



Table 10: The explicit representations of Euclidean differential invariants in  $DI_{(4,3)}^{IR}$ .

No	Expression	No	Expression
$DI_1$	$f_{20} + f_{02}$	$DI_2$	$f_{40} + 2f_{22} + f_{04}$
$DI_3$	$f_{10}^2 + f_{01}^2$	$DI_4$	$2f_{02}f_{20} - 2f_{11}$
$DI_6$	$f_{01}f_{03} + f_{01}f_{21} + f_{10}f_{12} + f_{10}f_{30}$	$DI_9$	$f_{01}f_{12} + f_{01}f_{30} - f_{10}f_{03} - f_{10}f_{21}$
$DI_{10}$	$f_{03}^2 + 3f_{12}^2 + 3f_{21}^2 + f_{30}^2$	$DI_{11}$	$2f_{03}f_{21} - 2f_{12}^2 + 2f_{12}f_{30} - 2f_{21}^2$
$DI_{13}$	$f_{04}^2 + 4f_{13}^2 + 6f_{22}^2 + 4f_{31}^2 + f_{40}^2$	$DI_{16}$	$f_{02}f_{04} + f_{02}f_{22} + 2f_{11}f_{13} + 2f_{11}f_{31} + f_{20}f_{22} + f_{20}f_{40}$
$DI_{20}$	$f_{02}f_{13} + f_{02}f_{31} - f_{04}f_{11} + f_{40}f_{11} - f_{13}f_{20} - f_{20}f_{31}$	$DI_{21}$	$2f_{04}f_{22} + 2f_{04}f_{40} - 2f_{13}^2 - 4f_{13}f_{31} + 2f_{22}^2 + 2f_{22}f_{40} - 2f_{31}^2$
$DI_{25}$	$f_{01}^2f_{02} + 2f_{01}f_{10}f_{11} + f_{10}^2f_{20}$	$DI_{26}$	$f_{01}^2f_{11} - f_{01}f_{02}f_{10} + f_{01}f_{10}f_{20} - f_{10}^2f_{11}$
$DI_{29}$	$4f_{04}f_{22}f_{40} - 4f_{04}f_{31}^2 - 4f_{13}^2f_{40} + 8f_{13}f_{22}f_{31} - 4f_{22}^3$	$DI_{30}$	$f_{01}^2f_{04} + f_{01}^2f_{22} + 2f_{01}f_{10}f_{13} + 2f_{01}f_{10}f_{31} + f_{10}^2f_{22} + f_{10}^2f_{40}$
$DI_{31}$	$f_{01}f_{02}f_{03} + 2f_{01}f_{11}f_{12} + f_{01}f_{20}f_{21} + f_{02}f_{10}f_{12} + 2f_{10}f_{11}f_{21} + f_{10}f_{20}f_{30}$	$DI_{33}$	$f_{01}^2f_{13} + f_{01}^2f_{31} - f_{01}f_{04}f_{10} + f_{01}f_{10}f_{40} - f_{10}^2f_{13} - f_{10}^2f_{31}$
$DI_{39}$	$f_{01}f_{02}f_{12} + 2f_{01}f_{11}f_{21} + f_{01}f_{20}f_{30} - f_{02}f_{03}f_{10} - 2f_{10}f_{11}f_{12} - f_{10}f_{20}f_{21}$	$DI_{44}$	$f_{02}^2f_{04} + 4f_{02}f_{11}f_{13} + 2f_{02}f_{20}f_{22} + 4f_{11}^2f_{22} + 4f_{11}f_{20}f_{31} + f_{20}^2f_{40}$
$DI_{45}$	$f_{01}f_{02}f_{03} + f_{01}f_{02}f_{21} + f_{01}f_{11}f_{12} + f_{01}f_{11}f_{30} + f_{03}f_{10}f_{11} + f_{10}f_{11}f_{21} + f_{10}f_{12}f_{20} + f_{10}f_{20}f_{30}$	$DI_{46}$	$f_{01}f_{03}f_{11} + f_{01}f_{11}f_{21} + f_{01}f_{12}f_{20} + f_{01}f_{20}f_{30} - f_{02}f_{03}f_{10} - f_{02}f_{10}f_{21} - f_{10}f_{11}f_{12} - f_{10}f_{11}f_{30}$
$DI_{48}$	$f_{02}f_{03}f_{30} - f_{02}f_{12}f_{21} - 2f_{03}f_{11}f_{21} - f_{03}f_{20}f_{30} + 2f_{11}f_{12}^2 + 2f_{11}f_{12}f_{30} - 2f_{11}f_{21}^2 + f_{12}f_{20}f_{21}$	$DI_{54}$	$f_{02}f_{03}^2 + 2f_{02}f_{12}^2 + f_{02}f_{21}^2 + 2f_{03}f_{11}f_{12} + 4f_{11}f_{12}f_{21} + 2f_{11}f_{21}f_{30} + f_{12}^2f_{20} + 2f_{20}f_{21}^2 + f_{20}f_{30}^2$
$DI_{62}$	$-f_{02}f_{03}f_{21} + f_{02}f_{12}^2 + f_{02}f_{12}f_{30} - f_{02}f_{21}^2 - 2f_{03}f_{11}f_{30} + f_{03}f_{20}f_{21} + 2f_{11}f_{12}f_{21} - f_{12}^2f_{20} - f_{12}f_{20}f_{30} + f_{20}f_{21}^2$	$DI_{78}$	$f_{01}f_{04}f_{12} + f_{01}f_{12}f_{22} + 2f_{01}f_{13}f_{21} + 2f_{01}f_{21}f_{31} + f_{01}f_{22}f_{30} + f_{01}f_{30}f_{40} - f_{03}f_{04}f_{10} - f_{03}f_{10}f_{22} - 2f_{10}f_{12}f_{13} - 2f_{10}f_{12}f_{31} - f_{10}f_{21}f_{22} - f_{10}f_{21}f_{40}$
$DI_{79}$	$f_{01}f_{03}f_{13} + f_{01}f_{03}f_{31} - f_{01}f_{04}f_{12} + f_{01}f_{12}f_{40} - f_{01}f_{13}f_{21} - f_{01}f_{21}f_{31} - f_{04}f_{10}f_{21} + f_{10}f_{12}f_{13} + f_{10}f_{12}f_{31} - f_{10}f_{13}f_{30} + f_{10}f_{21}f_{40}$	$DI_{83}$	$f_{01}f_{03}f_{22} + f_{01}f_{03}f_{40} + f_{01}f_{04}f_{21} - 2f_{01}f_{12}f_{13} - 2f_{01}f_{12}f_{31} + f_{01}f_{21}f_{22} + f_{04}f_{10}f_{30} + f_{10}f_{12}f_{22} + f_{10}f_{12}f_{40} - 2f_{10}f_{13}f_{21} - 2f_{10}f_{21}f_{31} + f_{10}f_{22}f_{30}$
$DI_{89}$	$f_{03}^2f_{04} + 4f_{03}f_{12}f_{13} + 2f_{03}f_{21}f_{22} + f_{04}f_{12}^2 + 4f_{12}^2f_{22} + 4f_{12}f_{13}f_{21} + 4f_{12}f_{21}f_{31} + 2f_{12}f_{22}f_{30} + 4f_{21}^2f_{22} + f_{21}^2f_{40} + 4f_{21}f_{30}f_{31} + f_{30}^2f_{40}$	$DI_{92}$	$-f_{02}f_{04}f_{22} + f_{02}f_{13}^2 + f_{02}f_{22}f_{40} - f_{02}f_{31}^2 - 2f_{04}f_{11}f_{31} + f_{04}f_{20}f_{22} + 2f_{11}f_{13}f_{22} - 2f_{11}f_{13}f_{40} + 2f_{11}f_{22}f_{31} - f_{13}^2f_{20} - f_{20}f_{22}f_{40} + f_{20}f_{31}^2$
$DI_{95}$	$-f_{03}f_{04}f_{21} - 2f_{03}f_{13}f_{30} + f_{03}f_{21}f_{40} - 2f_{03}f_{30}f_{31} + f_{04}f_{12}^2 + f_{04}f_{12}f_{30} - f_{04}f_{21}^2 - f_{12}^2f_{40} + 2f_{12}f_{13}f_{21} + 2f_{12}f_{21}f_{31} - f_{12}f_{30}f_{40} + f_{21}^2f_{40}$	$DI_{97}$	$-f_{04}^2f_{31} + 3f_{04}f_{13}f_{22} - f_{04}f_{13}f_{40} + 3f_{04}f_{22}f_{31} + f_{04}f_{31}f_{40} - 2f_{13}^2 - 2f_{13}^2f_{31} - 3f_{13}f_{22}f_{40} + 2f_{13}f_{31}^2 + f_{13}f_{40}^2 - 3f_{22}f_{31} + 2f_{31}^2$
$DI_{106}$	$-f_{02}f_{03}f_{12} - f_{02}f_{03}f_{30} - f_{02}f_{12}f_{21} - f_{02}f_{21}f_{30} + f_{03}^2f_{11} + 2f_{03}f_{11}f_{21} + f_{03}f_{12}f_{20} + f_{03}f_{20}f_{30} - f_{11}f_{12}^2 - 2f_{11}f_{12}f_{30} + f_{11}f_{21}^2$	$DI_{151}$	$f_{03}^2f_{04} + f_{03}^2f_{22} + f_{03}f_{04}f_{21} + 2f_{03}f_{12}f_{13} + 2f_{03}f_{12}f_{31} + 2f_{03}f_{21}f_{22} + f_{03}f_{21}f_{40} + f_{04}f_{12}^2 + f_{04}f_{12}f_{30} + f_{12}^2f_{22} + 4f_{12}f_{13}f_{21} + 4f_{12}f_{21}f_{31} + 2f_{12}f_{22}f_{30} + f_{12}f_{30}f_{40} + 2f_{13}f_{21}f_{30} + f_{21}^2f_{22} + f_{21}^2f_{40} + 2f_{21}f_{30}f_{31} + f_{22}f_{30}^2 + f_{30}^2f_{40}$

defined by Eq.(15) in Sect.2.5:

$$\begin{aligned}
& \frac{\partial^{i+j}G(x, y; \frac{\sigma}{\sqrt{2}})}{\partial x^i \partial y^j} \\
&= \frac{1}{\pi \sigma^2} \left(\frac{-1}{\sigma}\right)^{i+j} H_i\left(\frac{x-x_0}{\sigma}\right) H_j\left(\frac{y-y_0}{\sigma}\right) e^{-\frac{(x-x_0)^2+(y-y_0)^2}{\sigma^2}} \\
&= \frac{1}{\sqrt{\pi} \sigma} (2^{i+j} i! j!)^{\frac{1}{2}} \left(\frac{-1}{\sigma}\right)^{i+j} \hat{H}_i(x-x_0; \sigma) \hat{H}_j(y-y_0; \sigma) \\
&\quad \cdot e^{-\frac{(x-x_0)^2+(y-y_0)^2}{\sigma^2}}
\end{aligned}$$

(59)

When setting  $x_0=y_0=33$ ,  $\sigma = 12$ ,  $i, j \in \{0, 1, 2, 3, 4\}$  and  $1 \leq (i+j) \leq 4$ , we can find the images of  $\frac{\partial^{i+j}G(x, y; \frac{\sigma}{\sqrt{2}})}{\partial x^i \partial y^j}$  and  $\hat{H}_i(x-x_0; \sigma) \hat{H}_j(y-y_0; \sigma)$  are very similar, which are shown in Fig. 2a and Fig. 2b. Note that the size of each image is  $65 \times 65$  and the coordinate origin is at the upper left corner. In fact, the difference between them is entirely caused by  $e^{-\frac{(x-x_0)^2+(y-y_0)^2}{\sigma^2}}$ .

Therefore, we have reason to think that  $L_{ij}(x_0, y_0; \frac{\sigma}{\sqrt{2}})$  and  $\xi_{ij}^f(x_0, y_0; \sigma)$  extract almost the same information

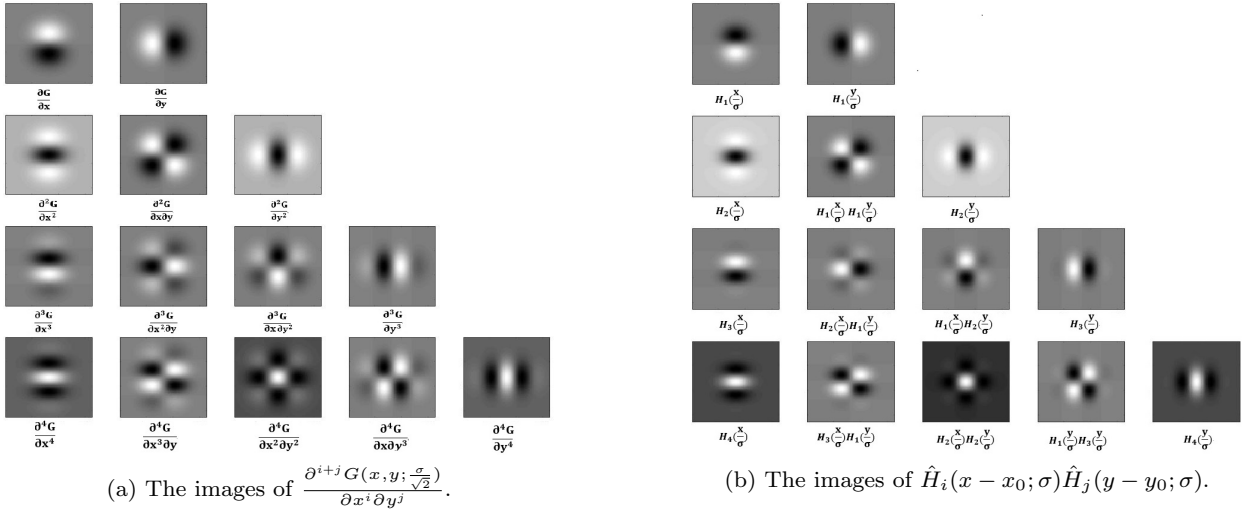


Fig. 2: The Relation between  $\frac{\partial^{i+j}G(x,y;\frac{\sigma}{\sqrt{2}})}{\partial x^i \partial y^j}$  and  $\hat{H}_i(x-x_0;\sigma)\hat{H}_j(y-y_0;\sigma)$  when  $i, j \in \mathbb{N}^+, 1 \leq (i+j) \leq 4$ .

about the image, where

$$\begin{aligned}
 L_{ij}(x_0, y_0; \frac{\sigma}{\sqrt{2}}) &= f \otimes A \frac{\partial^{i+j}G(x, y; \frac{\sigma}{\sqrt{2}})}{\partial x^i \partial y^j} \\
 &= A \sum_{y=1}^{y=M} \sum_{x=1}^{x=N} \frac{\partial^{i+j}G(x, y; \frac{\sigma}{\sqrt{2}})}{\partial x^i \partial y^j} f'(x, y) \\
 \xi_{ij}^f(x_0, y_0; \sigma) &= \sum_{y=1}^{y=M} \sum_{x=1}^{x=N} \hat{H}_i(x-x_0; \sigma) \hat{H}_j(y-y_0; \sigma) \\
 &\quad \cdot f(x, y)
 \end{aligned} \tag{60}$$

where  $A$  is a constant and  $f(x, y)$  can be transformed to  $f'(x, y)$  by horizontal and vertical flipping. In fact, using the symmetry of  $\frac{\partial^{i+j}G(x,y;\frac{\sigma}{\sqrt{2}})}{\partial x^i \partial y^j}$ , we have

$$\begin{aligned}
 L_{ij}(x_0, y_0; \frac{\sigma}{\sqrt{2}}) &= (-1)^{i+j} A \sum_{y=1}^{y=M} \sum_{x=1}^{x=N} \frac{\partial^{i+j}G(x, y; \frac{\sigma}{\sqrt{2}})}{\partial x^i \partial y^j} f(x, y) \\
 &= C \sum_{y=1}^{y=M} \sum_{x=1}^{x=N} \hat{H}_i(x-x_0; \sigma) \hat{H}_j(y-y_0; \sigma) e^{-\frac{(x-x_0)^2 + (y-y_0)^2}{\sigma^2}} \\
 &\quad \cdot f(x, y)
 \end{aligned} \tag{61}$$

where  $C$  is also a constant. Thus, when  $\sigma$  is relatively large,

$$L_{ij}(x_0, y_0; \frac{\sigma}{\sqrt{2}}) \approx \xi_{ij}^f(x_0, y_0; \sigma). \tag{62}$$

Recently, Yang and Flusser et al. (2011; 2013) found that the steerability of  $n$  order Gaussian-Hermite moments after 2D Euclidean transform is the same as that of  $n$  order central moments, which means image Gaussian-Hermite moment invariants can be generated by replacing central moments  $\eta_{ij}^f$  in geometric moment invariants with  $\xi_{ij}^f$ . As mentioned in Sect.2.5, Li et al. also used this method to construct image differential invariants. This indicates the isomorphism between differential invariants and Gaussian-Hermite moment invariants under 2D Euclidean transform also exists.

Based on this property and Eq.(62), image Gaussian-Hermite moment invariants can be regarded as differential invariants of discrete images when  $\sigma$  is large.

## 5.2 The Stability and Discriminability of Euclidean Differential Invariants

In order to evaluate the performance of Euclidean differential invariants, some synthesized databases are constructed. As shown in Fig. 3a, we select one image  $f(x, y)$  from the USC-SIPI texture database (<https://sipi.usc.edu/database.php?volume=textures>) and change its size to  $512 \times 512$ . As stated above, the coordinate system of  $(x, y)$  is located in the top left corner. Then, we choose 64 points  $(x_{k_1}, y_{k_2})$  in the domain of  $f(x, y)$  and crop the image patch  $f_{k_1, k_2}(x, y)$  in the  $65 \times 65$  neighborhood of each point  $(x_{k_1}, y_{k_2})$ , where  $x_{k_1} = 64(k_1 - 1) + 33$ ,  $y_{k_2} = 64(k_2 - 1) + 33$  and  $k_1, k_2 \in \{1, 2, \dots, 8\}$ . These image patches are shown in Fig. 3b. Finally, each patch  $f_{k_1, k_2}(x, y)$  is transformed to  $h_{k_1, k_2}^i(u, v)$  using the intensity affine transformation

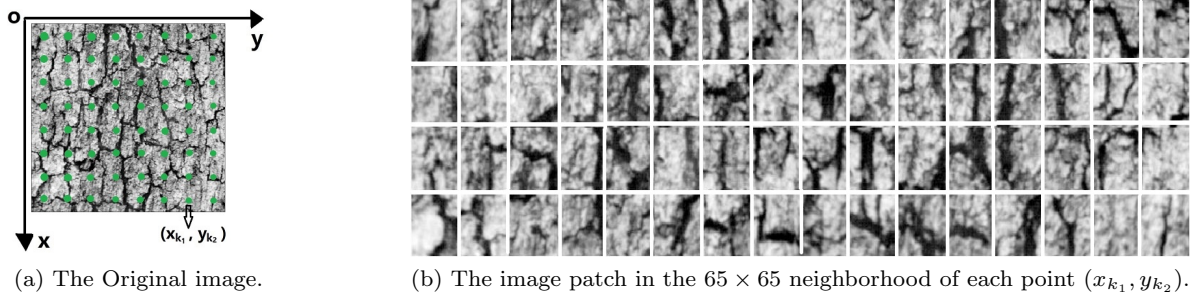


Fig. 3: The process to construct the synthesized database 1.

$h_{k_1, k_2}^i(u, v) = a_{k_1, k_2}^i f_{k_1, k_2}(x, y) + b_{k_1, k_2}^i$  and 2D rotation  $R_{k_1, k_2}^i$ , where  $a_{k_1, k_2}^i$ ,  $b_{k_1, k_2}^i$  and  $R_{k_1, k_2}^i$  are generated randomly,  $i \in \{1, 2, \dots, 60\}$ . This yields  $64 \cdot 60 = 3840$  images in the synthesized database 1.

In addition to intensity affine transform and 2D rotation, we define five image transforms in Table. 11 to simulate various noises. For each point  $(x_{k_1}, y_{k_2})$ , we translate it to  $(x_{k_1}^i, y_{k_2}^i) = (x_{k_1}^i + tx_{k_1, k_2}^i, y_{k_2}^i + ty_{k_1, k_2}^i)$ , where  $i \in \{1, 2, \dots, 60\}$ . The image patch  $f_{k_1, k_2}^i(x, y)$  in  $65s_{k_1, k_2}^i \times 65s_{k_1, k_2}^i$  neighborhood of  $(x_{k_1}^i, y_{k_2}^i)$  is cropped, where  $s_{k_1, k_2}^i$  is the scaling factor. Then,  $f_{k_1, k_2}^i(x, y)$  is transformed to  $h_{k_1, k_2}^i(u, v)$  using other transforms in Table. 11 and intensity affine transformation and 2D rotation. The size of  $h_{k_1, k_2}^i(u, v)$  is scaled to  $65 \times 65$ . We use 3840 images generated by this process to form the synthesized database 8. Note that all transformations mentioned above are generated randomly. By using different combinations of image transforms, we construct the synthesized database 2 (Rotation+Intensity Affine Transform+Translation), the synthesized database 3 (Rotation+Intensity Affine Transform+Translation+Scaling), the synthesized database 4 (Rotation+Intensity Affine Transform+Translation+Shear), the synthesized database 5 (Rotation+Intensity Affine Transform+Translation+Gaussian Noise), the synthesized database 6 (Rotation+Intensity Affine Transform+Intensity Power-Law Transform) and the synthesized database 7 (All transforms except the translation). Some example images in them are shown in Fig. 4.

We carry out classification experiments on these databases to evaluate the stability and discriminability of Euclidean differential invariants. For the synthesized database  $S$  ( $S \in \{1, 2, \dots, 8\}$ ), the first image  $h_{k_1, k_2}^1(u, v)$  from each of 64 categories is used as training data, and the rest 59 ones are used as testing data. Twelve independent sets  $DIS_{(O, D)}^I$  constructed in Table. 8 are employed as image features, where  $I \in \{LI, IR, FI\}$  and  $O, D \in \{3, 4\}$ . By convolving each image patch with the derivatives of 2D Gaussian function, we calculate numerical values of image partial deriva-

tives at the central point  $(33, 33)$ . The size of convolution kernel  $\frac{\partial^{i+j} G(x, y; \sigma)}{\partial x^i \partial y^j}$  is also  $65 \times 65$ . The standard deviation  $\sigma \in \{2, 4, \dots, 20\}$ . It should be noted that we standardize all image patches to zero mean and unit variance before we calculate invariants for them. This pre-processing operation can eliminate the effect of intensity affine transform. The magnitudes of numerical values of invariants in  $DIS_{(O, D)}^I$  are very different. Thus, the modified Chi-Square distance  $CSD$  is used to measure the similarity between two features  $X = (x_1, x_2, \dots, x_n)$  and  $Y = (y_1, y_2, \dots, y_n)$ :

$$CSD(X, Y) = \sum_{i=1}^{i=n} \frac{|x_i - y_i|}{|x_i| + |y_i|} \quad (63)$$

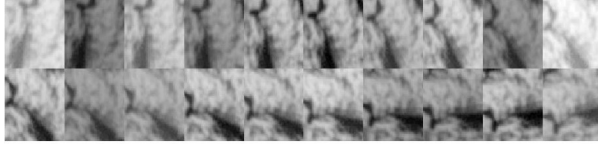
Note that  $0 \leq CSD(X, Y) \leq 1$ . We use a Nearest Neighbor classifier based on the modified Chi-Square distance to assign the class of the nearest model to each test image patch.

The classification accuracies from using various  $DIS_{(O, D)}^I$  on each synthesized database is shown Fig. 5. We observe that as long as the value of  $\sigma$  is set appropriately, each image feature can produce 100% accuracy on the database 1. Actually, the images  $h_{k_1, k_2}^1(u, v)$  and  $h_{k_1, k_2}^i(u, v)$  in this database are in rotation relation when the pre-processing operation mentioned in Sect. 5.2 have been done. Thus, for any Euclidean differential invariant  $DI$ , we have  $DI(h_{k_1, k_2}^1(u, v)) = DI(h_{k_1, k_2}^i(u, v))$  in theory. This property is called stability of invariants. In Fig. 6, the mean relative error ( $MRE$ ) is employed to test the stability of each Euclidean differential invariant  $DI_n$  in the set  $DI_{(4, 4)}^{LI}$ . When we set the value of the standard deviation  $\sigma$  and calculate  $DI_n$  on the database  $S$ ,  $MRE$  is defined by:

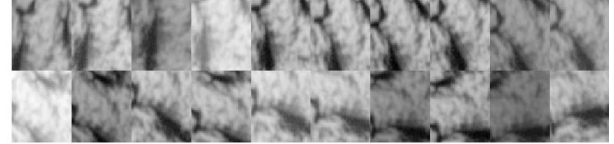
$$MRE_S^\sigma(DI_n) = \left( \frac{1}{64} \sum_{k_2=1}^{k_2=8} \sum_{k_1=1}^{k_1=8} \sum_{i=2}^{i=60} \frac{|DI_n(h_{k_1, k_2}^1) - DI_n(h_{k_1, k_2}^i)|}{|DI_n(h_{k_1, k_2}^1)| + |DI_n(h_{k_1, k_2}^i)|} \right) \times 100\%$$

Table 11: Five image transforms which are used to simulate various noises where  $k_1, k_2 \in \{1, 2, \dots, 8\}$  and  $i \in \{1, 2, \dots, 60\}$ .

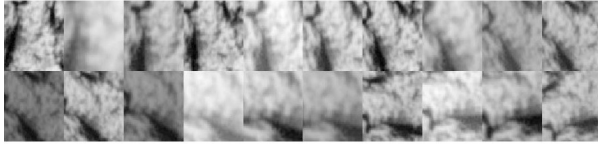
Transform	Definition	Parameter
Translation	$(x_{k_1}^i, y_{k_2}^i) = (x_{k_1} + tx_{k_1, k_2}^i, y_{k_2} + ty_{k_1, k_2}^i)$	$tx_{k_1, k_2}^i, ty_{k_1, k_2}^i \in [-10, 10]$
Scaling	$f_{k_1, k_2}^i(x, y) = f_{k_1, k_2}(s_{k_1, k_2}^i x, s_{k_1, k_2}^i y)$	$s_{k_1, k_2}^i \in [0.5, 1.5]$
Shear	$h_{k_1, k_2}^i(u, v) = f_{k_1, k_2}^i(x + mx_{k_1, k_2}^i y, y + my_{k_1, k_2}^i x)$	$mx_{k_1, k_2}^i, my_{k_1, k_2}^i \in [0, 0.3]$
Gaussian Noise	$h_{k_1, k_2}^i(u, v) = f_{k_1, k_2}^i(x, y) + N_{k_1, k_2}^i(x, y)$	$\sigma_{k_1, k_2}^i \in [0.001, 0.005]$
Intensity Power-Law Transform	$h_{k_1, k_2}^i(u, v) = (f_{k_1, k_2}^i(x, y))^{\alpha_{k_1, k_2}^i}$	$\alpha_{k_1, k_2}^i \in [0.5, 2]$



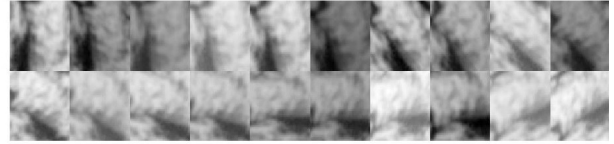
The Synthesized Database 1  
(Rotation+Intensity Affine Transform)



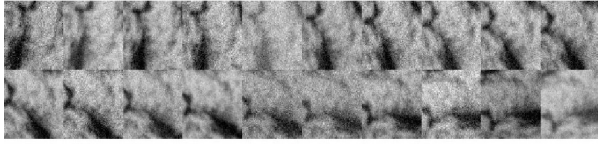
The Synthesized Database 2  
(Rotation+Intensity Affine Transform+Translation)



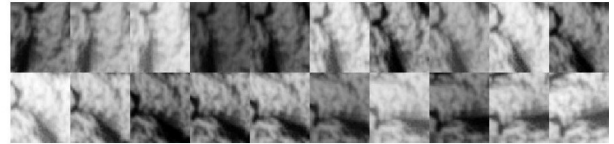
The Synthesized Database 3  
(Rotation+Intensity Affine Transform+Scaling)



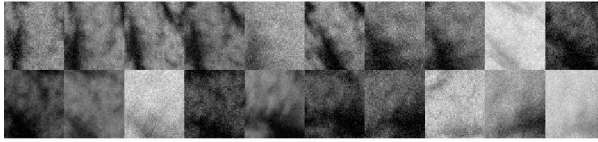
The Synthesized Database 4  
(Rotation+Intensity Affine Transform+Shear)



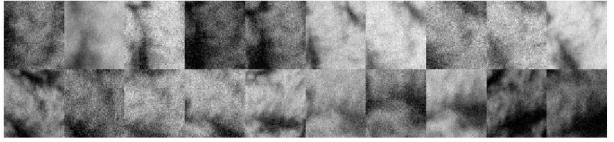
The Synthesized Database 5  
(Rotation+Intensity Affine Transform+Gaussian Noise)



The Synthesized Database 6  
(Rotation+Intensity Affine Transform+Intensity Power-Law Transform)



The Synthesized Database 7  
(Rotation+Intensity Affine Transform+Scaling+Shear  
+Gaussian Noise+Intensity Power-Law Transform)



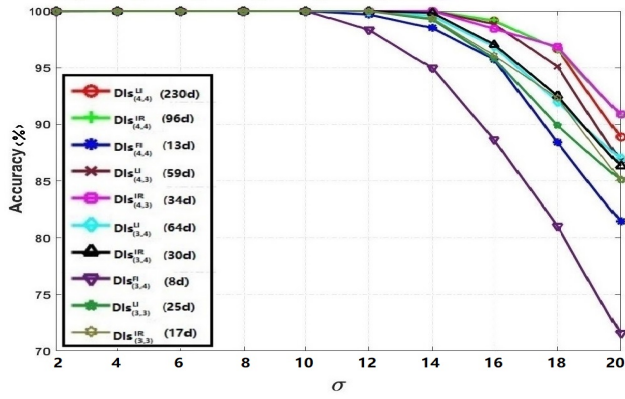
The Synthesized Database 8  
(Rotation+Intensity Affine Transform+Translation+Scaling+Shear  
+Gaussian Noise+Intensity Power-Law Transform)

Fig. 4: Some example images in the synthesized database 1 ~ 8.

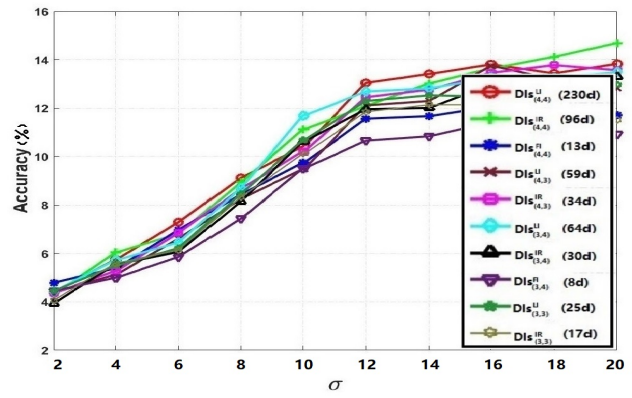
(64)

where  $n \in \{1, 2, \dots, 230\}$ ,  $S \in \{1, 2, \dots, 8\}$  and  $\sigma \in \{2, 4, \dots, 20\}$ . Note that  $0\% \leq MRE_S^\sigma(DI_n) \leq 100\%$ . The results show both  $MRE_1^6(DI_n)$  and  $MRE_1^8(DI_n)$  are less than 10% for any  $n$ . Thus, the numerical value of  $DI_n$  remains basically the same when the image is transformed using 2D Euclidean transform. However, their stability drops significantly when image patches are disturbed by various transforms in Table. 11. It can be observed that  $40\% \leq MRE_2^\sigma(DI_n) \leq 90\%$ ,  $40\% \leq MRE_3^\sigma(DI_n) \leq 75\%$ ,  $20\% \leq MRE_4^\sigma(DI_n) \leq 60\%$ ,

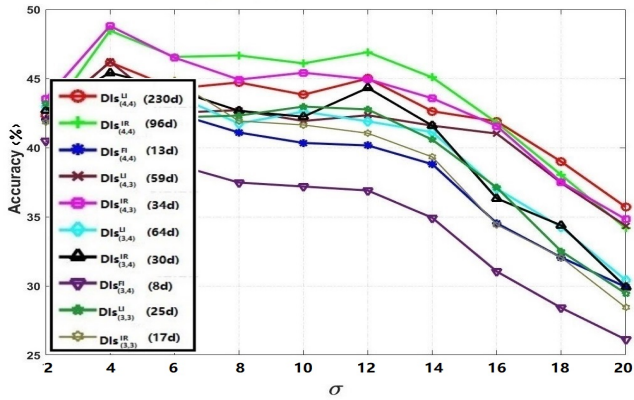
$10\% \leq MRE_5^\sigma(DI_n) \leq 40\%$  and  $10\% \leq MRE_6^\sigma(DI_n) \leq 40\%$  for most  $n$  and  $\sigma$ . This is because the local structure in  $f_{k_1, k_2}^i(x, y)$  has been changed. For example, the image patch in  $65 \times 65$  neighborhood of the point  $(x_{k_1}, y_{k_2})$  must be different from that of the point  $(x_{k_1} + tx_{k_1, k_2}^i, y_{k_2} + ty_{k_1, k_2}^i)$  when  $tx_{k_1, k_2}^i$  and  $ty_{k_1, k_2}^i$  are relatively large. In fact, the translation transform has the most serious impact on the stability of  $DI_n$  because the highest classification accuracy on the synthesized database 2 is only 14.86%. The difference in classification accuracy on the database 7 and 8 also indicates this point. Compare to geometric transforms (Translation, Scaling and Shear),



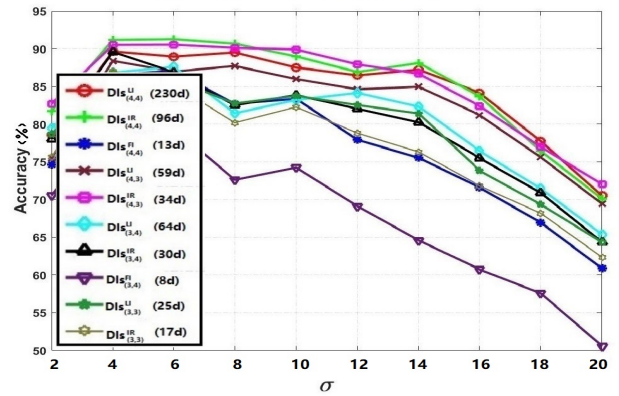
The Synthesized Database 1



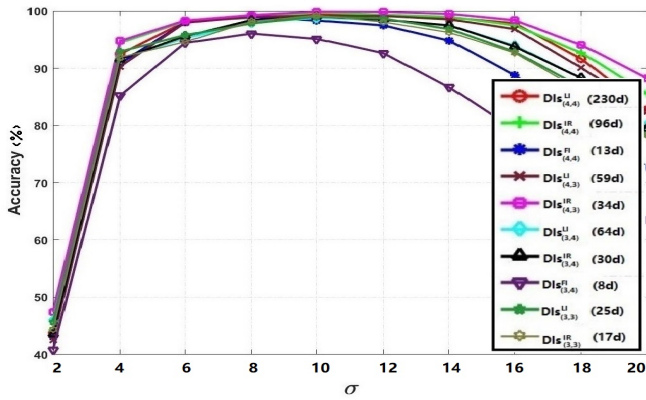
The Synthesized Database 2



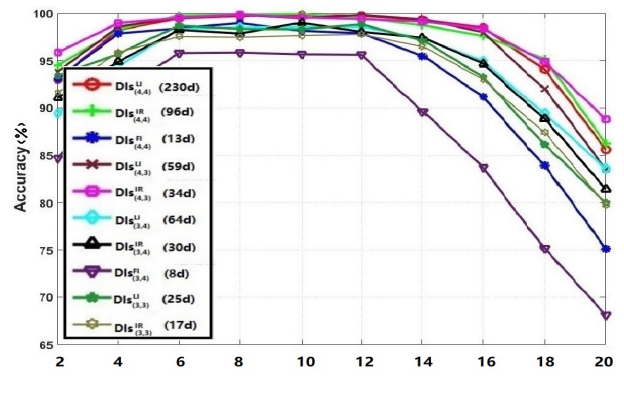
The Synthesized Database 3



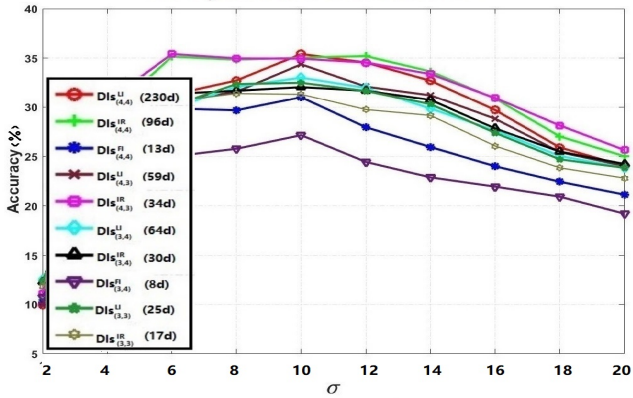
The Synthesized Database 4



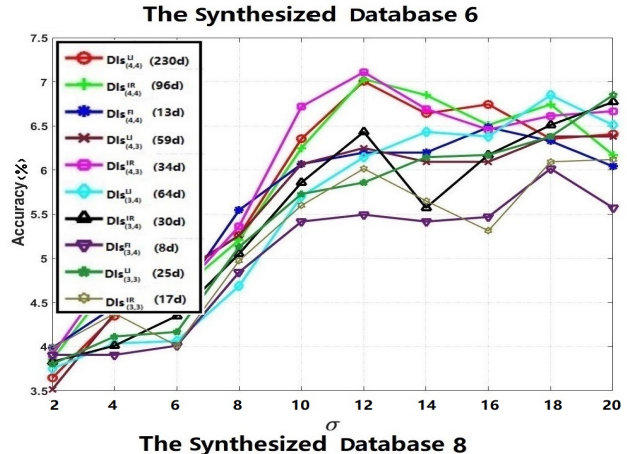
The Synthesized Database 5



The Synthesized Database 6



The Synthesized Database 7



The Synthesized Database 8

Fig. 5: The classification accuracies on synthesized databases when various independent sets of Euclidean differential invariants are used as image features.

intensity transforms (Intensity Power-Law Transform and Gaussian Noise) have less influence on the stability of Euclidean differential invariants. For example, when setting  $\sigma = 12$ , the highest classification accuracy on the synthesized database 5 and 6 is also 100%.

We also find the accuracy from using any  $DI s_{(O,D)}^I$  on each database increases first and then declines as  $\sigma$  gradually changes from 2 to 20. In most cases, the highest accuracy is acquired by setting  $\sigma = 12$ . As stated previously, the size of every convolution kernel is also  $65 \times 65$ . According to  $3\sigma$  rule of thumb, we should set  $\sigma = \frac{65}{6} \approx 11$  to ensure that nearly 100% values of  $\frac{\partial^{i+j} G(x,y;\sigma)}{\partial x^i \partial y^j}$  lie within the  $65 \times 65$  square neighborhood of the point (33, 33). Another interesting observation is that the performance of  $DI s_{(O,D)}^{IR}$  is better than  $DI s_{(O,D)}^{LI}$  and  $DI s_{(O,D)}^{FI}$ , where  $O, D \in \{3, 4\}$ . This is because the number of invariants in  $DI s_{(O,D)}^{FI}$  is too small to distinguish image patches belonging to different categories. And the invariants in  $DI s_{(O,D)}^{LI}$  which can be expressed as the polynomials of others not only do not extract new information about the image, but introduce computational errors. In addition, the accuracy from using  $DI s_{(4,D)}^I$  is higher than that from using  $DI s_{(3,D)}^I$ , where  $I \in \{LI, IR, FI\}$  and  $D \in \{3, 4\}$ . This is due to the forth-order partial derivatives extracting more image information. However,  $DI s_{(O,3)}^I$  performs better than  $DI s_{(O,3)}^I$ , where  $I \in \{LI, IR, FI\}$  and  $O \in \{3, 4\}$ . Actually, the higher the degree, the more easily the numerical value of the differential invariant is disturbed by image transforms in Table. 11.

### 5.3 Image Patch Verification on the HPatches Database

The HPatches database consists of  $65 \times 65$  image patches which are cropped from various image sequences and organized into pairs (Balntas et al. 2017). An image sequence include a reference image and 5 target images with varying real geometric and intensity transforms. For image patch verification, image features are employed to classify whether two patches in correspondence (positive pairs) or not (negative pairs). In order to increase the difficulty of this task, the patches are disturbed by random generated easy (E), hard (H) and tough (T) image transforms, including intensity and geometric transforms. Some example patches in the database are shown in Fig. 7. And negative pairs can be formed by patches from the same image sequence (Intra) and from different image sequences (Inter). Actually, the ones from the same image sequence are considered more challenging as the textures in different regions of the image are often similar.

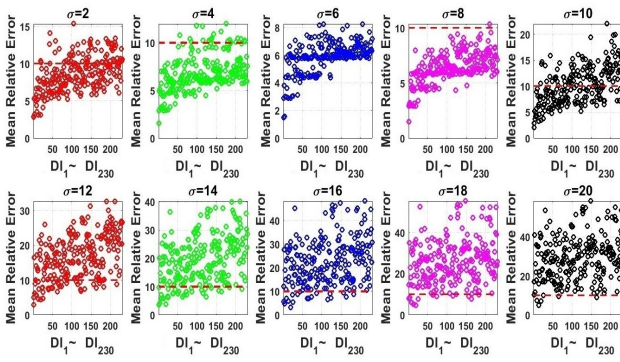
Image patch verification is carried out on 72 sub-databases (E+Intral:12, E+Inter:12, H+Intral:12, H+Inter:12, T+Intral:12, T+Inter:12), each containing  $2 \times 10^5$  positive pairs and  $1 \times 10^6$  negative pairs. Similar to the process described in Sect.5.2,  $DI s_{(O,D)}^I$  is calculated at central point (33, 33) on each image patch and used as image feature, where  $I \in \{LI, IR, FI\}$  and  $O, D \in \{3, 4\}$ . We follow the standard evaluation protocol provided by the authors and replace the Euclidean distance with the modified Chi-Square distance defined by Eq.(63) to measure the similarity between two image patches. The mean average precision(mAP) is employed to evaluate the performance of various image features.

The experimental results are shown in Fig. 8. We omitted the mAP from using  $DI s_{(4,4)}^{FI}$  and  $DI s_{(3,4)}^{FI}$  because  $DI s_{(4,4)}^{FI} = DI s_{(4,3)}^{FI}$  and  $DI s_{(3,4)}^{FI} = DI s_{(3,3)}^{FI}$ . It can be observed these results are consistent with the classification experiments in Sect.5.2. For example, the mAP from using  $DI s_{(4,3)}^{IR}$  is higher than others for any  $\sigma$ , and most features achieve optimal performance when setting  $\sigma = 12$ .

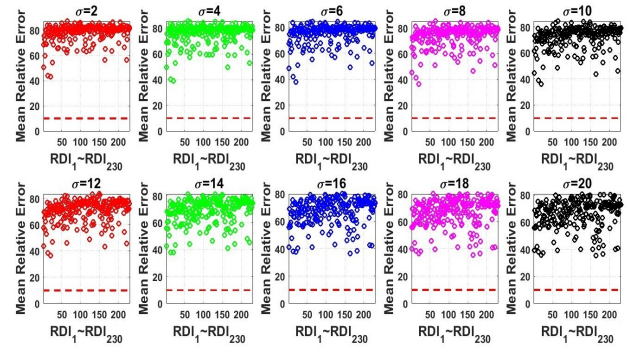
In addition to  $DI s_{(O,D)}^I$ , seven famous handcrafted features are chosen for benchmark, including SIFT (128d) (David 2004), RootSIFT (128d) (Arandjelović and Zisserman 2012), ORB (256d) (Rublee et al. 2011), BRIEF (256d) (Calonder et al. 2012), BinBoost (256d) (Trzcinski et al. 2014),  $J^3$  (9d) and  $J^4$  (14d). Note that  $J^N$  represents the local jet of order  $N$ . In order to increase difficulty of verification, we conduct experiments on 12 (T+Intra) subdatabases. Only the highest mAP from using  $DI s_{(O,D)}^I$ ,  $J^3$  and  $J^4$  is displayed when  $\sigma$  increases from 2 to 20. As shown in Fig. 9, we find the performance of  $DI s_{(4,3)}^{IR}$  is superior to almost all other image features when image patches are deformed by tough image transforms. It should be pointed out the state-of-the-art approach, BinBoost, is constructed by using a complicated learning framework and its dimension is 7 times that of  $DI s_{(4,3)}^{IR}$ . Thus, the computational cost of  $DI s_{(O,D)}^I$  is lower than that of BinBoost.

### 5.4 Texture Image Classification on the CUREt Database

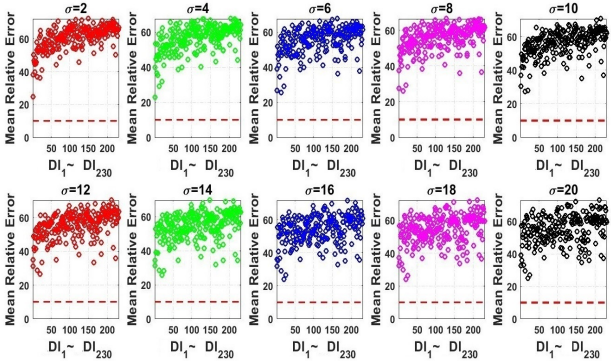
The experiments are designed to test the classification of texture images. We use the CUREt database available at [www.robots.ox.ac.uk/~vgg/research/texclass/setup.html](http://www.robots.ox.ac.uk/~vgg/research/texclass/setup.html). This database contains 61 texture classes with 92 images per class. The size of each image is  $200 \times 200$ . Forth-six images used as training data are randomly selected from each of 61 classes, and the rest images are used as testing data. Also, we use the pre-



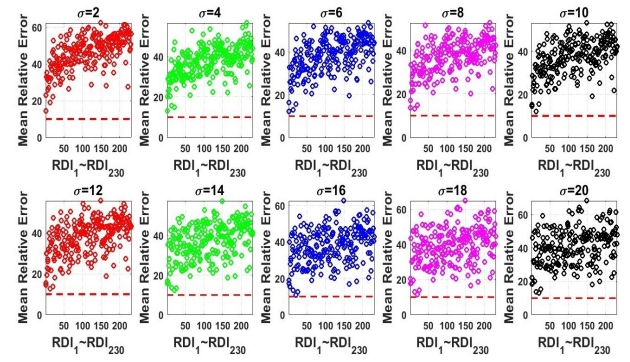
The Synthesized Database 1



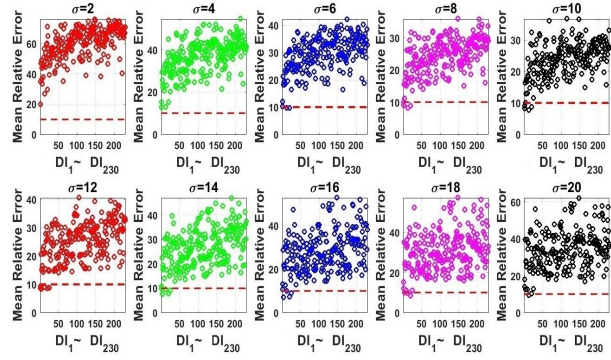
The Synthesized Database 2



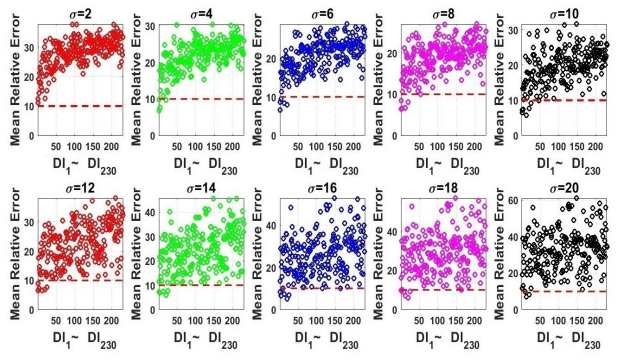
The Synthesized Database 3



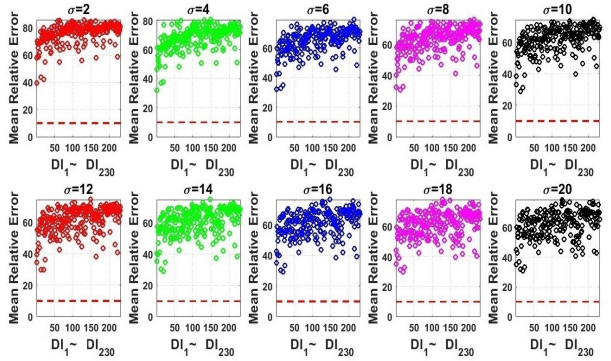
The Synthesized Database 4



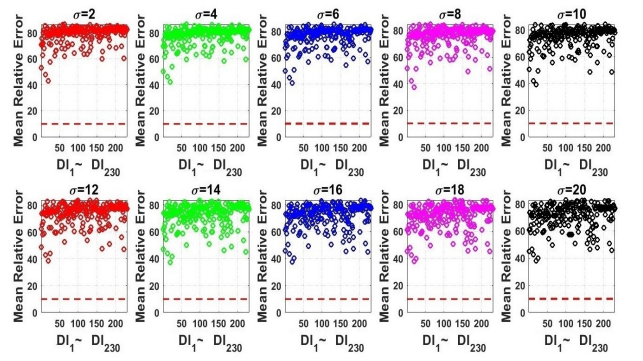
The Synthesized Database 5



The Synthesized Database 6



The Synthesized Database 7



The Synthesized Database 8

Fig. 6: The MRE of  $DI_n$  in  $DI_s^{LI}_{(4,4)}$  on the synthesized database 1 ~ 8, when setting the standard deviation  $\sigma \in \{2, 4, \dots, 20\}$ .

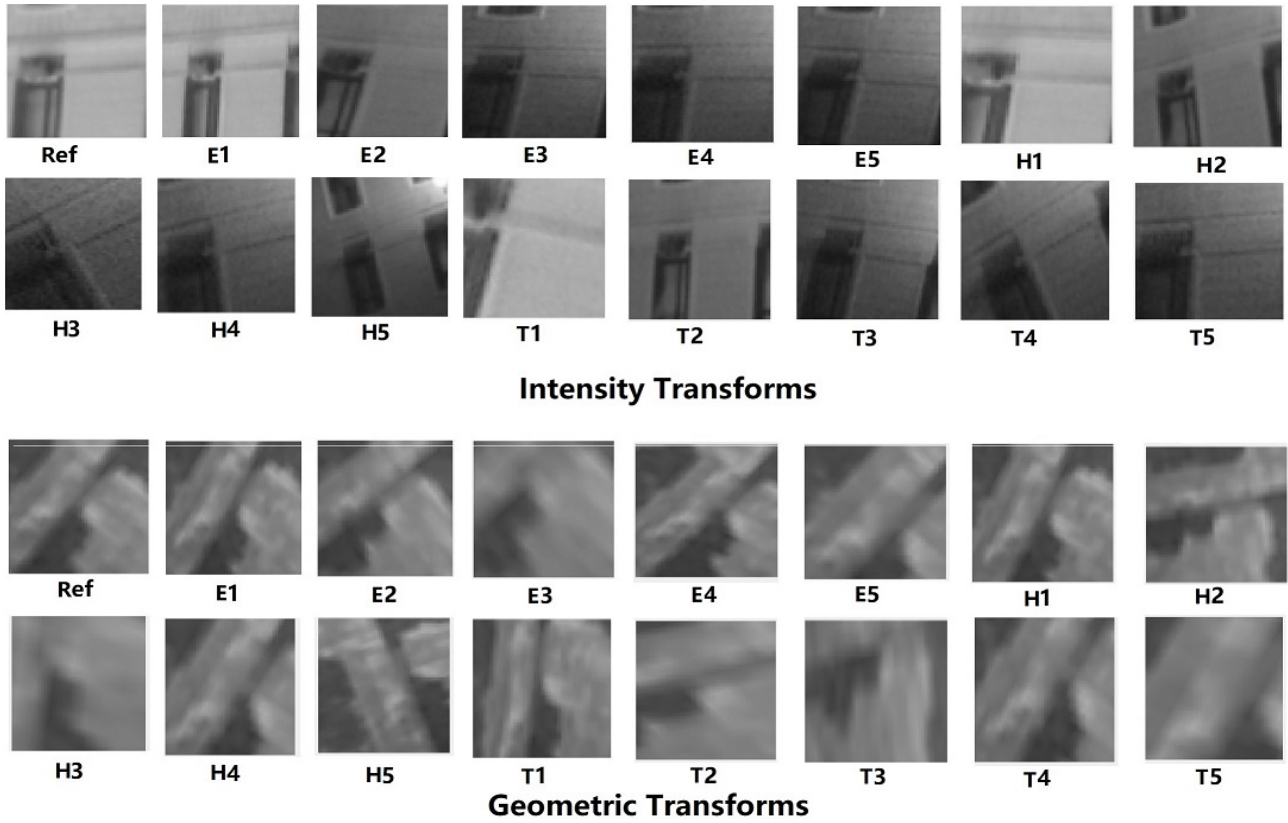


Fig. 7: Some example images in the HPatches database.

processing operation to normalize these images. On the image  $f(x, y) : \Omega \subset \mathbb{N}^+ \times \mathbb{N}^+ \rightarrow \mathbb{R}$ , we calculate 9 image features at each point  $(x_0, y_0) \in \Omega$ . These features are:

- **LBP<sup>riu2</sup><sub>24,3</sub>** (26d) (Ojala et al. 2002): Twenty-four points  $(x_0^k, y_0^k)$  are sampled around a circle of radius 3 centred at  $(x_0, y_0)$ , where  $k \in \{1, 2, \dots, 24\}$ . The values of  $f(x_0^k, y_0^k)$  and  $f(x_0, y_0)$  are used to construct the rotation-invariant uniform pattern of the point  $(x_0, y_0)$ . A 26-dimensional histogram can be obtained using the pattern on each point.
- **BIF** (1296d) (Crosier and Griffin 2010): As mentioned in Sect. 3.1, BIF consists of six functions of three Euclidean differential invariants  $DI_1$ ,  $DI_2$  and  $DI_3$  defined in Table. 1. If the value of the  $i$ th function at  $(x_0, y_0)$  is larger than others, this point is labelled as  $i$  where  $i \in \{1, 2, \dots, 6\}$ . The derivatives of 2D Gaussian function  $G(x, y; \sigma)$  are used to calculate image partial derivatives. And a 4-dimensional image feature can be obtained at each point  $(x, y) \in \Omega$  when setting  $\sigma = 1, 2, 4, 8$ . This feature has a total of  $6^4 = 1296$  possible values. Thus, we can get a 1296-dimensional histogram on each image.
- **LETRIST** (413d) (Song et al. 2018): Similar to BIF, three complicated functions of  $DI_1$ ,  $DI_2$  and  $DI_3$  in Table. 1 are used to describe the local structure in the neighborhood of each point  $(x_0, y_0)$ . The values of image partial derivatives at  $(x_0, y_0)$  are also obtained by convoluting the image with the Gaussian derivative filters. The standard deviation  $\sigma = 1, 2, 4$ . A 413-dimensional histogram can be constructed based on the feature.
- **VZ-MR8** (8d) (Varma and Zisserman 2005): This method extracts image information in the neighborhood of  $(x_0, y_0)$  using the MR8 filter bank and generates a 8-dimensional image feature at each point. This feature is invariant under 6 special rotation transformations.
- **VZ-Joint** (49d) (Varma and Zisserman 2009): The image patch in the  $7 \times 7$  square neighborhood of  $(x_0, y_0)$  is used to describe local structure. This resulting 49-dimensional feature is not invariant under 2D Euclidean transform.
- **S-C** (13d) (Schmid 2001): The responses of thirteen filters which are circular symmetry are used to construct the feature at each point  $(x_0, y_0)$ .
- **CMR** (8d) (Zhang et al. 2013): Zhang et al. use the maximum values of the first and second direc-



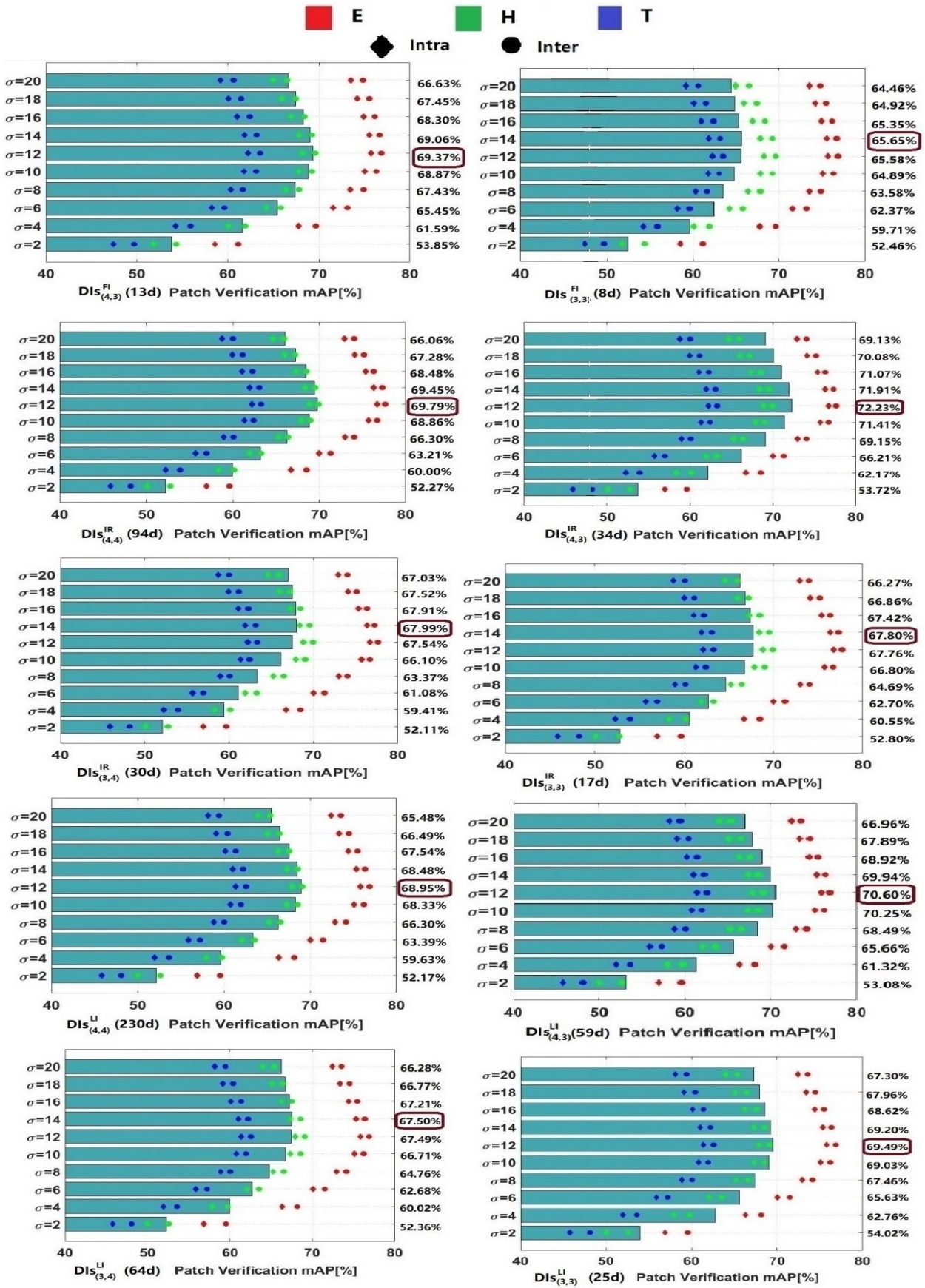


Fig. 8: The mAP from using  $DIS_{(O,D)}^I$  on the HPatches database where  $I \in \{LI, IR, FI\}$  and  $O, D \in \{3, 4\}$ .

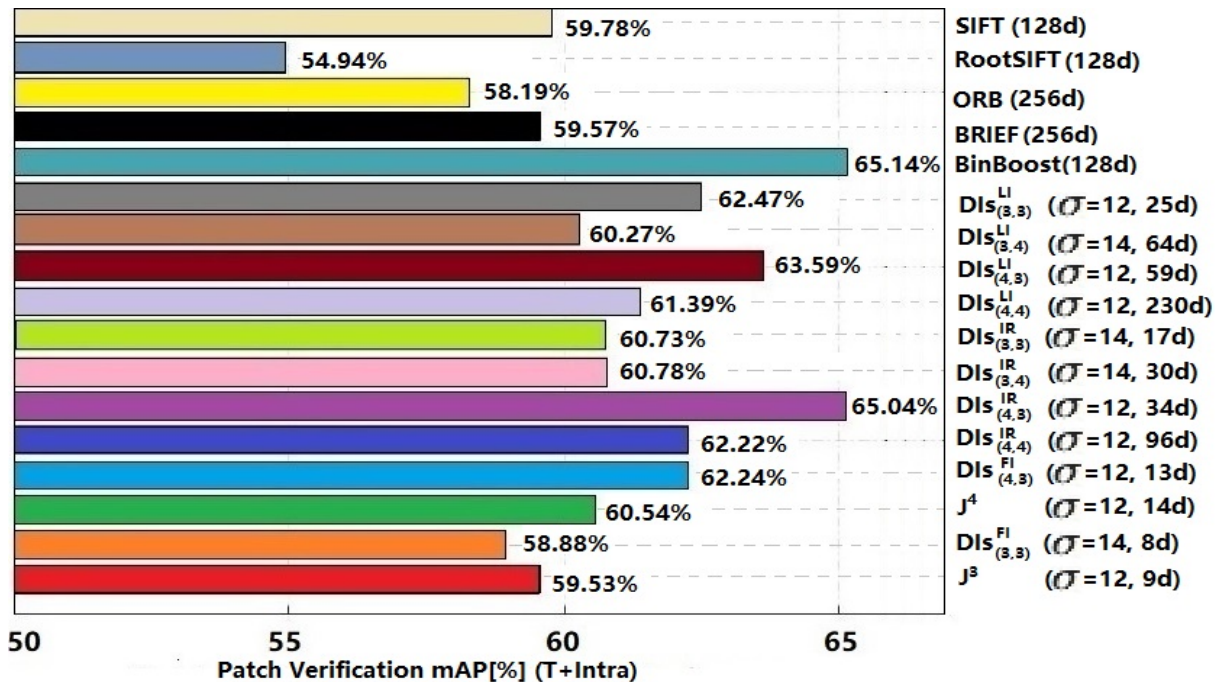


Fig. 9: The mAP from using various image features on 12 (T+Intra) subdatabases.

tional derivatives defined by Eq.(25) in Sect.3.1 to construct a 8-dimensional image feature at  $(x_0, y_0)$  when setting  $\sigma = 1, 2, 4, 8$ . We have pointed out that these maximum values can be expressed as the functions of  $DI_1$ ,  $DI_2$  and  $DI_3$  in Table. 1.

- $J^2$  (15d): The local jet of the order 2,  $J(x_0, y_0; \sigma)$ , is calculated at each point  $(x_0, y_0)$ . When setting the standard deviation  $\sigma = 1, 2, 4, 8$ , we can get a 20-dimensional image feature at  $(x_0, y_0)$ . Note that  $J^2$  is also not invariant under 2D Euclidean transform.
- **DI**s (12d): Unlike BIF, LETRIST and CMR, we use  $DI_1$ ,  $DI_2$  and  $DI_3$  defined in Table. 1 directly to describe the image local structure in the neighborhood of  $(x_0, y_0)$ . Also, we estimate the numerical values of image partial derivatives at  $(x_0, y_0)$  by convoluting the image with the derivatives of  $G(x, y; \sigma)$ . A 12-dimensional image feature can be acquired when the standard deviation  $\sigma$  is set to 1, 2, 4 and 8.

It should be noted that VZ-MR8, VZ-Joint, S-C, CMR,  $J^2$  and DI

s can only be used to extract the information at each point  $(x_0, y_0) \in \Omega$ . In order to describe the overall information of  $f(x, y)$ , we use the procedure proposed by Varma and Zisserman to construct histograms based on these features. First, thirteen images are chosen randomly for each texture. The image features over all these images are clustered using K-Means to produce 10 texton cluster centres per class. Note that the Euclidean distance used in the standard

K-Means is replaced with the modified Chi-Square distance when we calculate the cluster centres of DI

s and  $J^2$ . Then, we get the texton dictionary which contains  $10 \cdot 61 = 610$  textons. Finally, we use these textons to label each point in the image  $f(x, y)$  and obtain the 610-dimensional histogram of texton frequencies.

The Nearest Neighbor classifier based on the Chi-Square distance is used for classification. By repeating the classification experiment with 100 different random selections of training and test data, the mean accuracy from using each feature along with the standard deviation is shown in Table. 12. We find the performance of LETRIST, BIF, CMR and DI

s is better than that from using others. As mentioned above, these image features are all constructed by using Euclidean differential invariants  $DI_1$ ,  $DI_2$  and  $DI_3$  in Table. 1. An interesting observation is that the classification accuracy from using DIs ( $97.92 \pm 0.71\%$ ) is higher than that using CMR ( $97.67 \pm 0.64\%$ ). This seems to indicate that we do not have to construct the complicated functions of  $DI_1$ ,  $DI_2$  and  $DI_3$  when we use the texton-based approach described above to construct image histograms.

Surprisingly,  $J^2$ , which are not invariant under 2D Euclidean transform, also performs very well ( $97.86 \pm 0.60\%$ ). In fact, the CURET database is not suitable to evaluate the invariance of image features for the action of 2D Euclidean transformation group, because images have no significant rotation. To address this we transform each image in the CURET database using

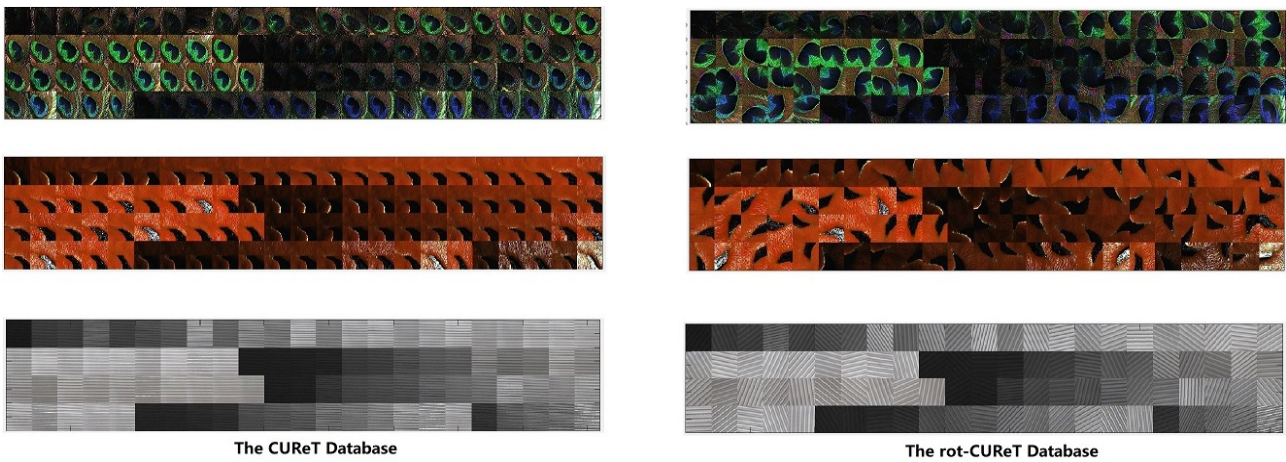


Fig. 10: Some texture classes in the CURET database and the rot-CURET database.

a random generated rotation transformation. The rot-CURET database consist of these transformed images. Some texture classes in the CURET database and the rot-CURET database are shown in Fig. 10. We repeat the experiment on the rot-CURET database and get the classification accuracy from using various image features.

Obviously, the accuracy from using VZ-Joint and  $J^2$  on the new database drops by more than 20%. We find the classification accuracy from using DIs ( $97.14 \pm 0.80\%$ ) is better than that using BIF ( $96.69 \pm 0.62\%$ ) and CMR ( $96.84 \pm 0.77\%$ ). And the best performance is achieved by using LETRIST ( $97.66 \pm 0.65\%$ ), consistent with the experimental results on the CURET database. This implied that we should pay attention to directly constructing histograms based on image differential invariants rather than using the texton dictionary to generate them. Furthermore, it can be predicted that we can get higher classification accuracy on these databases by using more Euclidean differential invariants.

## 6 Conclusion and Future Work

In this paper, we design two fundamental differential operators to generate homogeneous polynomials of image partial derivatives, which are absolute or relative invariant under 2D Euclidean, similarity and affine transforms. They are called as image differential invariants. When setting the degree of the polynomial and the order of image partial derivatives are less than or equal to 4, we generate all Euclidean differential invariants and derive various independent sets of them.

When using the derivatives of 2D Gaussian function to estimate image partial derivatives, we propose

the relation between Euclidean differential invariants and Gaussian-Hermite moment invariants. Image classification and verification are carried out on some synthesized and real image databases. Based on the experimental results, we analyse the effect of various factors on the performance of Euclidean differential invariants in detail. Also, these differential invariants perform better than commonly used handcrafted image features in most cases.

In the future, we plan to analyse the geometric meaning of higher order differential invariants and construct effective image handcrafted features based on them. In addition, the feature maps obtained by using Euclidean differential invariants in  $DI_{(4,3)}^{IR}$  are shown in Fig. 8 when  $\sigma$ , the standard deviation of 2D Gaussian function is set to 8. Obviously, they extract abundant information about image local structure. We may be able to use them as inputs of convolutional neural networks to improve the accuracy of image classification and retrieval.

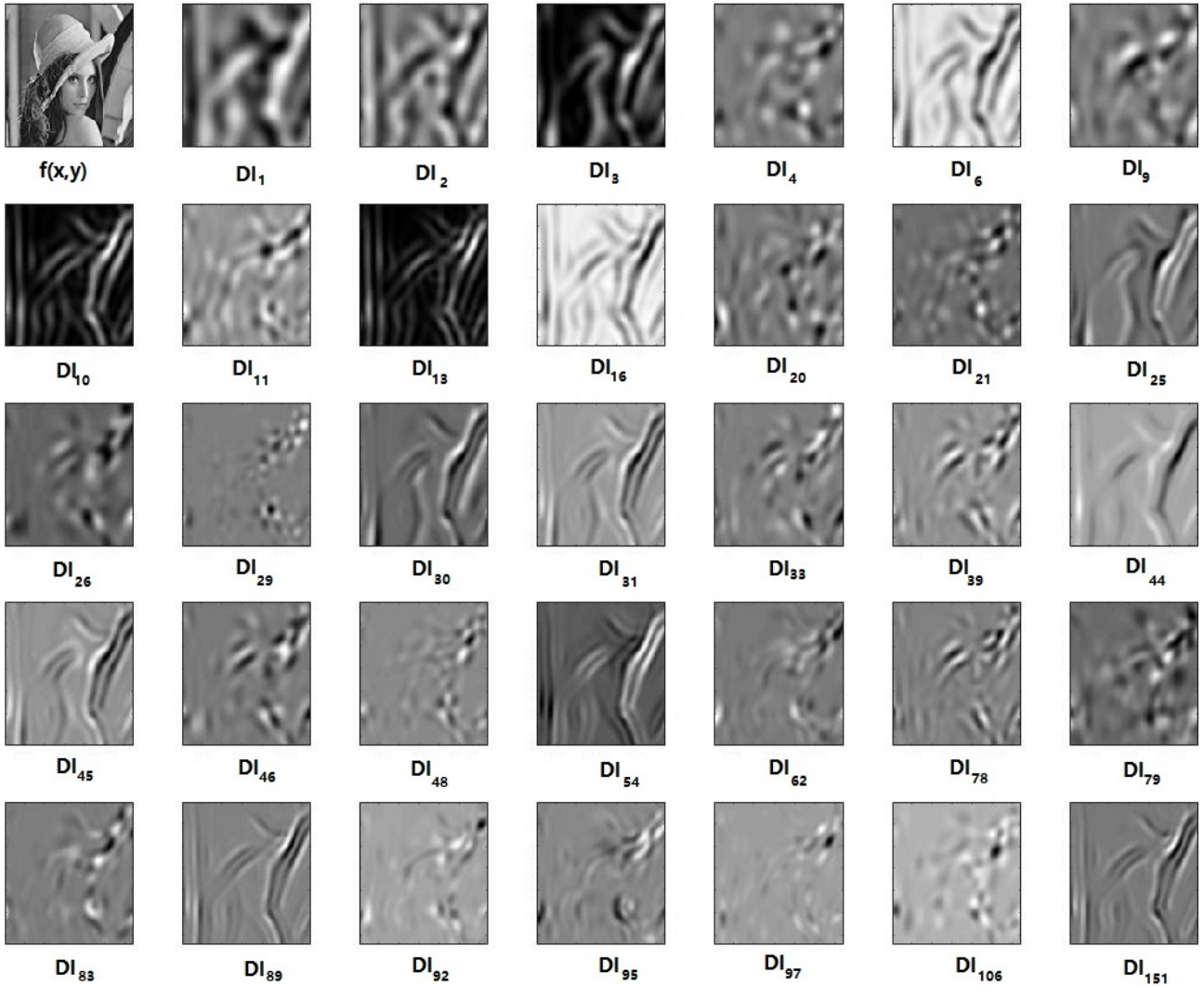
**Acknowledgements** This work has partly been funded by the National Key R&D Program of China (No. 2017YFB1002703) and the National Natural Science Foundation of China (Grant No. 60873164, 61227802 and 61379082).

## References

- Arandjelović, R., & Zisserman, A. (2012). Three things everyone should know to improve object retrieval. In *CVPR* (pp. 2911-2918).
- Baltas, V., Lenc, K., Vedaldi, A., & Mikolajczyk, K. (2017). HPatches: A benchmark and evaluation of handcrafted and learned local descriptors. In *CVPR* (pp. 5173-5182).
- Brown, A.,B. (1935). Functional dependence. *Transactions of American Mathematical Society*, 38(2), 379-394.
- Calabi, E., Olver, P. J., Shakiban, C., Tannenbaum, A., & Haker, S. (1998). Differential and numerically invariant

Table 12: The classification accuracy from using various image features on the CURET database and the rot-CURET database.

Image Feature	Accuracy (CURET)	Accuracy (rot-CURET)
LBP <sub>24,3</sub> <sup>iu2</sup> (26d)	87.08 ± 1.12%	71.88 ± 1.13%
BIF (1296d)	<b>98.03±0.51%</b>	<b>96.69±0.62%</b>
LETRIST (413d)	<b>98.59±0.50%</b>	<b>97.66±0.65%</b>
VZ-MR8 (610d)	97.33 ± 0.71%	95.67 ± 0.94%
VZ-Joint (610d)	96.20 ± 0.77%	72.48 ± 0.98%
S-C (610d)	95.53 ± 1.16%	93.71 ± 1.19%
CMR (610d)	<b>97.67±0.64%</b>	<b>96.84±0.77%</b>
J <sup>2</sup> (610d)	97.86 ± 0.60%	72.48 ± 1.01%
DIs (610d)	<b>97.92±0.71%</b>	<b>97.14±0.80%</b>

Fig. 11: The feature maps obtained by using Euclidean differential invariants in  $DI_{(4,3)}^{IR}$  when the standard deviation of 2D Gaussian function is 8.

- signature curves applied to object recognition. *IJCV*, 26(2), 107-135.
- Calonder, M., Lepetit, V., Ozuysal, M., Trzcinski, T., Strecha, C., & Fua, P. (2012). BRIEF: Computing a local binary descriptor very fast. *IEEE TPAMI*, 34(7), 1281-1298.
- Cartan, É. (1935). *La Méthode du Repère Mobile, la Théorie des Groupes Continus, et les Espaces Généralisés*. Exposés de Géométrie No. 5, Hermann, Paris.
- Crosier, M., & Griffin, L. D. (2010). Using basic image features for texture classification. *IJCV*, 88(3), 447-460.
- David, G. L. (2004). Distinctive image features from scale-invariant keypoints. *IJCV*, 60(2), 99-110.
- Florack, L. M. J., ter Haar Romeny, B. M., Koenderink, J. J., & Viergever, M. A. (1992). Scale and the differential structure of images. *Image and Vision Computing*, 10(6), 376-388.
- Florack, L. M. J., ter Haar Romeny, B. M., Koenderink, J. J., & Viergever, M. A. (1993). Cartesian differential invariants in scale-space. *Journal of Mathematical Imaging and Vision*, 3(4), 327-348.
- Florack, L. M. J., ter Haar Romeny, B. M., Koenderink, J. J., & Viergever, M. A. (1994). General intensity transformations and differential invariants. *Journal of Mathematical Imaging and Vision*, 4(2), 171-187.
- Florack, L. M. J., & Balmashnova, E. (2008). Novel similarity measures for differential invariant descriptors for generic object retrieval. *Journal of Mathematical Imaging and Vision*, 31(2-3), 121-132.
- Flusser, J., & Suk, T. (1993). Pattern recognition by affine moment invariants. *Pattern Recognition*, 26(1), 167-174.
- Flusser, J. & Suk, T. (1994). A moment-based approach to registration of images with affine geometric distortion. *IEEE Transactions on Geoscience and Remote Sensing*, 32(2), 382C387.
- Freeman, W. T., & Adelson, E. H. (1991). The design and use of steerable filters. *IEEE TPAMI*, 13(9), 891-906.
- Gong, M., Hao, Y., Mo, H. L., Li, H. (2017). Naturally combined shape-color moment invariants under affine transformations. *CVIU*, 162, 46-56.
- Griffin, L. D. (2007). The second order local-image-structure solid. *IEEE TPAMI*, 29(8), 1355-1366.
- Griffin, L. D., Lillholm, M., Crosier, M., & van Sande, J. (2009). Basic image features (BIFs) arising from approximate symmetry type. In *Scale space and variational methods in computer vision* (pp. 343C355).
- Griffin, L. D., & Lillholm, M. (2010). Symmetry sensitivities of derivative-of-gaussian filters. *IEEE TPAMI*, 32(6), 1072C1083.
- Griffin, L. D. (2019). The atlas structure of images. *IEEE TPAMI*, 41(1), 234-245.
- Heikkilä, J. (2004). Pattern matching with affine moment descriptors. *Pattern Recognition*, 37(9), 1825C1834.
- Hu, M. K. (1962). Visual pattern recognition by moment invariants. *IEEE Transactions on Information and Theory*, 8(2), 179-187.
- Karakasis, E. G., Amanatiadis, A., Gasteratos, A. & Chatzichristofis, S. A. (2015). Image moment invariants as local features for content based image retrieval using the Bag-of-Visual-Words model. *Pattern Recognition Letters*, 55(1), 22-27.
- Koenderink, J. J., & van Doorn, A. J. (1987). Representation of local geometry in the visual system. *Biological Cybernetics*, 55(6), 367-375.
- Koenderink, J. J., & van Doorn, A. J. (1992). Surface shape and curvature scales. *Image and Vision Computing*, 10(8), 557-564.
- Li, E. B., & Li, H. (2017). Isomorphism between differential and moment invariants under affine transform. ArXiv preprint [arXiv:1705.08264](https://arxiv.org/abs/1705.08264)
- Li, E. B., Huang, Y. Z., Xu, D., & Li, H. (2017). Shape DNA: basic generating functions for geometric moment invariants. ArXiv preprint [arXiv:1703.02242](https://arxiv.org/abs/1703.02242)
- Li, E. B., Mo, H. L., Xu, D., & Li, H. (2018). Image Projective Invariants. *IEEE TPAMI*, 41(5), 1144-1157.
- Lie, S. (1884). Über Differentialinvarianten. *Mathematische Annalen*, 24(4), 537-578.
- Lindeberg, T. (1994). On scale selection for differential operators. In *Scale-Space Theory in Computer Vision*, 256, 317-348.
- Lindeberg, T., & Gårding, J. (1997). Shape-adapted smoothing in estimation of 3-D shape cues from affine deformations of local 2-D brightness structure. *Image and Vision Computing*, 15(6), 415-434.
- Mikolajczyk, K., & Schmid, C. (2001). Indexing based on scale invariant interest points. In *ICCV* (Vol. 1, pp. 525-531).
- Mikolajczyk, K., & Schmid, C. (2004). Scale and affine invariant interest point detectors. *IJCV*, 60(1), 63-86.
- Mikolajczyk, K., & Schmid, C. (2005). A performance evaluation of local descriptors. *IEEE TPAMI*, 27(10), 1615C1630.
- Mikolajczyk, k., Tuytelaars, T., Schmid, C., Zisserman, A., Matas, J., Schaffalitzky, F., Kadir, T., & Van Gool, L. (2005). A comparison of affine region detectors. *IJCV*, 65(1-2), 43-72.
- Mukundan, R., Ong, S. H., & Lee, P. A. (2001). Image analysis by Tchebichef moments. *IEEE TIP*, 10(9), 1357-1364.
- Ojala, T., Pietikainen, M., & Maenpaa, T. (2002). Multiresolution gray-scale and rotation invariant texture classification with local binary patterns. *IEEE TPAMI*, 24(7), 971-987.
- Olver, P. J. (1995). *Equivalence, Invariants, and Symmetry*. Cambridge University Press.
- Olver, P. J., Sapiro, G., & Tannenbaum, A. (1999). Affine invariant detection: edge maps, anisotropic diffusion, and active contours. *Acta Applicandae Mathematica*, 59(1), 45-77.
- Olver, P. J. (1999). *Classical invariant theory*. Cambridge University Press.
- Olver, P. J. (2015). Moving Frame Derivation of the Fundamental Equi-Affine Differential Invariants for Level Set Functions. Preprint [http://www-users.math.umn.edu/~%20olver/mf\\_eals.pdf](http://www-users.math.umn.edu/~%20olver/mf_eals.pdf)
- Reiss, T. H. (1991). The revised fundamental theorem of moment invariants. *IEEE TPAMI*, 13(8), 830C840.
- Rublee, E., Rabaud, V., Konolige, K., & Bradski, G. (2011). ORB: An efficient alternative to SIFT or SURF. In *ICCV* (pp. 2564-2571).
- Salden, A. H., ter Haar Romeny, B. M., Florack, L. M. J., Viergever, M. A., & Koenderink, J. J. (1992). A complete and irreducible set of local orthogonally invariant features of 2-dimensional images. In *IAPR International Conference on Pattern Recognition* (Vol. 3, pp. 180-184)
- Schmid, C. (2001). Constructing models for content-based image retrieval. In *CVPR* (Vol. 2, pp. 39-45).
- Schmid, C., & Mohr, R. (1997). Local grayvalue invariants for image retrieval. *IEEE TPAMI*, 19(5), 530-535.
- Sheng, Y., & Shen, L. (1994) Orthogonal Fourier-Mellin moments for invariant pattern recognition. *Journal of the Optical Society of America A*, 11(6), 1748C1757.

- Song, T. C., Meng, F. M., Wu, Q. B., Luo, B., Zhang, T. Q., & Xu, Y. J. (2017). L2SSP: Robust keypoint description using local second-order statistics with soft-pooling. *Neurocomputing*, 230, 230-242.
- Song, T. C., Li, H. L., Meng, F. M., Wu, Q. B., & Cai, J. F. (2018). LETRIST: Locally encoded transform feature histogram for rotation-invariants texture classification. *IEEE TCSVT*, 28(7), 1565-1579.
- Suk, T., & Flusser, J. (2004). Graph method for generating affine moment invariants. In *ICPR (Vol 2)*, pp. 192-195.
- Teague, M., R. (1980). Image analysis via the general theory of moments. *Journal of the Optical Society of America*, 70(8), 920-930.
- Ter Haar Romeny, B. M., Florack, L. M. J., Salden, A. H., & Viergever, M. A. (1994). Higher Order Differential Structure of Images. *Image and Vision Computing*, 12(6), 317-325.
- Tresse, A. (1894). Sur les invariants différentiels des groupes continus de transformations. *Acta Mathematica*, 18(1), 1-88, 1894.
- Trzcinski, T., Christoudias, M., & Lepetit, V. (2014). Learning image descriptors with Boosing. *IEEE TPAMI*, 37(3), 597-610.
- Tuznik, S. L., Olver, P. J., & Tannenbaum, A. (2018). Equi-affine differential invariants for invariant feature point detection. *European Journal of Applied Mathematics*, <https://doi.org/10.1017/S0956792519000020>
- Varma, M., & Zisserman, A. (2005). A statistical approach to texture classification from single images. *IJCV*, 62(1-2), 61-81.
- Varma, M., & Zisserman, A. (2009). A statistical approach to material classification using image patch exemplars. *IEEE TPAMI*, 31(11), 2032C2047.
- Xu, D., & Li, Hua. (2008). Geometric moment invariants. *Pattern Recognition*, 41(1), 240-249.
- Yang, B., & Dai, M. (2011). Image analysis by Gaussian-Hermite moments. *Signal Processing*, 91(10), 2290-2303.
- Yang, B., Kostková, J., Flusser, J., & Suk, T. (2011). Scale invariants from Gaussian-Hermite moments. *Signal Processing*, 132, 77-84.
- Yang, B., Li, G. X., Zhang, H. L., & Dai, M. (2011). Rotation and translation invariants of Gaussian-Hermite moments. *Pattern Recognition Letters*, 32(9), 1283-1298.
- Yang, B., Flusser, J., & Suk, T. (2013). Steerability of hermite kernel. *International Journal of Pattern Recognition and Artificial Intelligence*, 27(4), 1-25.
- Zhang, J., Zhao, H., & Liang, J. M. (2013). Continuous rotation invariant local descriptors for texton dictionary-based texture classification. *CVIU*, 117(1), 56-75.